Mon. Not. R. Astron. Soc. **000**, 1–?? (2009) Printed 13 January 2013 (MN LaTeX style file v2.2)

arXiv:1103.0024v2 [astro-ph.GA] 18 Jul 2011

The population of Milky Way satellites in the ΛCDM cosmology

A. S. Font,[1,3⋆] A. J. Benson[2], R. G. Bower[3], C. S. Frenk[3], A. Cooper[3,9], G. DeLucia[4], J. C. Helly[3] A. Helmi[5], Y.-S. Li[5,6], I. G. McCarthy[1,7], J. F. Navarro[8], V. Springel[10,11], E. Starkenburg[5], J. Wang[3], and S. D. M. White[9]

[1] *Institute of Astronomy, University of Cambridge, Madingley Road, Cambridge, CB3 0HA*
[2] *California Institute of Technology MC 350-17, 1200 E. California Blvd., Pasadena, CA 91125, U.S.A.*
[3] *Institute of Computational Cosmology, Department of Physics, University of Durham, Science Laboratories, South Road, Durham DH1 3LE*
[4] *INAF-Osservatorio Astronomico di Trieste, Via Tiepolo 11, I-34131 Trieste, Italy*
[5] *Kapteyn Astronomical Institute, University of Groningen, PO Box 800, 9700 AV Groningen, the Netherlands*
[6] *Kavli Institute for Astronomy and Astrophysics, Peking University, Beijing 100871, China*
[7] *Kavli Institute for Cosmology, University of Cambridge, Madingley Road, Cambridge, CB3 OHA*
[8] *University of Victoria, 3800 Finnerty Road, Victoria, BC V8P 5C2, Canada*
[9] *Max Planck Institut für Astrophysik Karl-Schwarzschild-Str. 1 85741 Garching, Germany*
[10] *Heidelberg Institute for Theoretical Studies, Schloss-Wolfsbrunnenweg 35, 69118 Heidelberg, Germany*
[11] *Zentrum für Astronomie der Universität Heidelberg, Astronomisches Recheninstitut, Mönchhofstr. 12-14, 69120 Heidelberg, Germany*

Accepted ... Received ...

ABSTRACT

We present a model for the satellites of the Milky Way in which galaxy formation is followed using semi-analytic techniques applied to the six high-resolution N-body simulations of galactic halos of the Aquarius project. The model, calculated using the GALFORM code, incorporates improved treatments of the relevant physics in the ΛCDM cosmogony, particularly a self-consistent calculation of reionization by UV photons emitted by the forming galaxy population, including the progenitors of the central galaxy. Along the merger tree of each halo, the model calculates gas cooling (by Compton scattering off cosmic microwave background photons, molecular hydrogen and atomic processes), gas heating (from hydrogen photoionization and supernova energy), star formation and evolution. The evolution of the intergalactic medium is followed simultaneously with that of the galaxies. Star formation in the more massive progenitor subhalos is suppressed primarily by supernova feedback, while for smaller subhalos it is suppressed primarily by photoionization due to external and internal sources. The model is constrained to match a wide range of properties of the present day galaxy population as a whole, but at high redshift it requires an escape fraction of UV photons near unity in order completely to reionize the universe by redshift $z \gtrsim 8$. In the most successful model the local sources photoionize the pre-galactic region completely by $z \simeq 10$. In addition to the luminosity function of Milky Way satellites, the model matches their observed luminosity-metallicity relation, their radial distribution and the inferred values of the mass within 300 pc, which in the models increase slowly but significantly with luminosity. There is a large variation in satellite properties from halo to halo, with the luminosity function, for example, varying by a factor of ~ 2 among the six simulations.

Key words: Galaxy: evolution — Galaxy: formation — galaxies: dwarf

1 INTRODUCTION

A basic prediction of the cold dark matter (CDM) theory of structure formation is that galactic dark matter halos grow by the accretion and disruption of smaller subsystems. A

⋆ E-mail: `afont@ast.cam.ac.uk`

well-known consequence of this is that the Milky Way today should be surrounded by thousands of small subhalos, in apparent contradiction with the much smaller number of luminous satellites that have been detected around the Milky Way so far. This has been termed the 'missing satellite problem' (Klypin et al. 1999; Moore et al. 1999). A second potential discrepancy with the theory is the recent observation by Strigari et al. (2008) that the satellites of the Milky Way all have very similar central densities even though they span five orders of magnitude in luminosity, suggesting the existence of a preferred scale which is not present, for example, in the primordial cold dark matter power spectrum of density perturbations.

It has long been recognized that the reionization of the intergalactic medium (IGM) by the metagalactic UV radiation field at early times can inhibit the formation of small galaxies (Couchman & Rees 1986; Efstathiou 1992; Thoul & Weinberg 1996). It has also been recognized for some time that this process would provide at least part of the solution to the missing satellite problem (Kauffmann et al. 1993; Bullock, Kravtsov & Weinberg 2000; Benson et al. 2002b; Somerville 2002). Bullock, Kravtsov & Weinberg (2000), in particular, emphasized the vital role of early reionization and calculated a simple model for the abundance of satellites in the CDM cosmogony. Since reionization imposes a scale in the problem—a minimum entropy for the reionized hydrogen—this process may also solve the second 'satellite problem' (Li et al. 2009; Okamoto & Frenk 2009; Stringer et al. 2010).

Galaxy formation in small halos can also be strongly inhibited by winds generated by the injection of supernova energy into the gas (White & Rees 1978). The combined effects of this so-called "supernova feedback" and early reionization were used by Kauffmann et al. (1993) to explain the relative paucity of satellite galaxies around the Milky Way, and modelled in greater detail by Benson et al. (2002b) who showed that this relatively simple physics could account not only for the abundance of the 'classical satellites', but also for many of the properties known at the time, such as gas content, metallicity and star formation rate. The Benson et al. (2002b) model predicted the existence of many more satellites in the Local Group. A few years later, a new population of satellites was discovered, through careful searches of the Sloan Digital Sky Survey, more than doubling the number of known satellites around the Milky Way (Willman et al. 2005; Zucker et al. 2006; Belokurov et al. 2007; Irwin et al. 2007; Walsh et al. 2007; see also Martin et al. 2004). The luminosity function of the newly found satellites matches the theoretical predictions remarkably well (Koposov et al. 2008).

The discovery of a new population of ultra-faint satellites led to renewed interest in the physics of dwarf galaxy formation. A number of recent studies have revisited the arguments of the 1990s and early 2000s, either using semi-analytic modelling techniques (Cooper et al. 2010; Guo et al. 2011a; Li et al. 2010; Macciò et al. 2010), or simpler models (Koposov et al. 2009; Busha et al. 2010; Muñoz et al. 2009), generally confirming the conclusions of the earlier work. Some of these studies (Busha et al. 2010; Muñoz et al. 2009; Cooper et al. 2010) have taken advantage of a new generation of high resolution N-body simulations which track the formation of galactic halos and their surviving subhalos down to the smallest halos likely to support the formation of faint galaxies (Diemand, Kuhlen & Madau 2007; Springel et al. 2008b). This allows calculation of the expected radial distribution of satellites which was not predicted with sufficient precision by the semi-analytic approach of Benson et al. (2002b), based on Monte-Carlo halo merger trees and an analytic model of satellite orbital evolution. In addition to these semi-analytic calculations, full N-body/gasdynamic simulations of galaxies and their satellites have now been carried out (Libeskind et al. 2007; Okamoto & Frenk 2009; Okamoto et al. 2010; Wadepuhl & Springel 2011). These too find that reionization plays a key role in suppressing dwarf galaxy formation but, as stressed by Kauffmann et al. (1993), feedback from supernova energy is also a major factor. Wadepuhl & Springel (2011) find, further, that cosmic ray pressure is also important in suppressing star formation in these galaxies.

Although a consensus seems to be emerging then, that the abundance and other properties of the Milky Way satellites can be understood as a consequence of the known physics of galaxy formation in a ΛCDM universe, a number of important uncertainties remain. For example, Boylan-Kolchin et al. (2011) have recently concluded, on the basis of dynamical data, that the most massive subhalos in N-body simulations are too concentrated to be able to host the brightest satellites of the Milky Way. There are also significant modelling uncertainties. Recent studies treat reionization in a simplified way (Busha et al. 2010; Koposov et al. 2009; Macciò et al. 2010; Busha et al. 2010; Guo et al. 2011a; Li et al. 2010), reducing this complex process to a simple rule involving a few adjustable parameters (e.g., a single redshift for reionization and a threshold mass above which reionization is unimportant). Furthermore, the luminosity function is just one of many observables that depend critically on the assumed physics of the problem. The metallicity of the satellites, for example, not considered in most of these studies, is very sensitive to the effects of supernova feedback.

In this paper, we investigate the formation of satellite galaxies in the ΛCDM cosmogony employing a new treatment of reionization, based on that of Benson et al. (2002a), that simultaneously solves for the coupled evolution of the galaxy population and the IGM. The ionizing background is computed from the integrated emission history of all galaxies in the Universe plus a simple model for the quasar contribution, filtered through the optical depth of the IGM whose evolution and ionization state are computed self-consistently. The ionizing radiation, generated by galaxies and quasars, feeds back upon subsequent galaxy formation through the dual action of photoionization, which *i)* prevents the collapse of gas onto low mass dark matter halos and *ii)* reduces the rate of radiative cooling inside more massive halos. An original feature of this model is the inclusion of internal reionization from progenitors of the Milky Way.

Since the early work on satellite galaxies a decade ago, there have been important developments in techniques for modelling galaxy formation. Many of these have been incorporated into the Durham semi-analytic model, GALFORM (Cole et al. 2000; Bower et al. 2006), which we use in this paper. To this, we add treatments of cooling and heating processes that are relevant on the scale of dwarf galaxies. In addition to the usual atomic radiative processes, we include cooling due to molecular hydrogen (H_2) and Compton cooling of gas due to scattering off cosmic microwave background photons. Heating due to photoionization is calculated using CLOUDY (Ferland et al. 1998). The evolution of the IGM is computed taking into account the contribution of the UV ionizing background from both galaxies and quasars. The emissivity from galaxies is calculated self-consistently, whereas the contribution from quasars is modelled using an updated version of the spectrum inferred observationally by Haardt & Madau (1996). The model then predicts the time dependence of the properties of the IGM, such as its mean temperature and ionization state which, in turn, determine the rate at which it cools into galaxies.

We find that, in addition to the global UV background pervading the Universe, the radiation generated locally by stars forming in the progenitors of the Milky Way is an important source of ionization in the Milky Way at early times. As we will demonstrate, this radiation increases the redshift of reionization locally and leads to a stronger suppression of satellite galaxy formation than the metagalactic flux. Recently, Muñoz et al. (2009) have identified this mechanism of ‘inside out reionization’ of the Milky Way as important in suppressing the formation of ultra-faint dwarfs. According to these authors, self-reionization occurs much before the time when the Universe as a whole was reionized, at an epoch when most of the gas was in molecular (H_2) form. They suggest that reionization would quench cooling of the H_2 gas, stopping it from fragmenting and forming stars, possibly explaining the paucity of ultra-faint dwarfs today. In practice, they model this process by making similar assumptions to those made in simple models of the effects of global reionization, namely by assuming that H_2 cooling becomes ineffective below a given halo mass after a given redshift. By contrast, we implement the self-reionization of the Milky Way by explicitly calculating the UV flux produced by the progenitors of the Milky Way as a function of time. This takes away any freedom in the choice of redshift and halo mass for which this process is important, while the same is achieved concomitantly for the global reionization with the self-consistent approach.

In this paper, we implement our model of the coupled evolution of galaxies and the IGM in merger trees constructed from the high resolution simulations of galactic halos in the Aquarius project (Springel et al. 2008a). The resolution of these simulations (with particle masses ranging from 6.4×10^3 to $1.4 \times 10^4 M_\odot$) is sufficient to enable predictions to be made for satellites as faint as even the faintest dwarfs detected recently around the Milky Way. Using the six Aquarius simulations, we can investigate halo-to-halo variations in the properties of the satellites.

Our method for simulating the joint evolution of galaxies and the IGM, as well as the new physics we have implemented in GALFORM, are explained in Section 2. In Section 3, we demonstrate how the metallicity−luminosity relation of satellites can be used to break the model degeneracy between the effects of supernova feedback and reionization. We also explore how self-reionization changes the predicted abundance of satellites. We find, however, that it is not possible for the model simultaneously to match the luminosity function and the metallicity−luminosity relation with the default supernova feedback prescription used in previous implementations of GALFORM, in which the efficiency of the feedback increases with decreasing halo size as a power-law. Instead, the satellite data require that this feedback efficiency should saturate for halos with circular velocity, $v_{\rm circ} \leqslant 65$ km s^{-1}. In Section 4, we test this model further by considering predictions for the radial distribution of satellites and for the mass within 300 pc. Finally, in Section 5, we discuss our conclusions and carry out a comparison with the results by Li et al. (2010) using similar semi-analytic techniques. A detailed comparison with other related models is presented in Appendix B.

The cosmological parameters adopted in this study are the same as those used for the Aquarius and Millennium (Springel et al. 2005) simulations and correspond to a flat ΛCDM cosmology with matter density, $\Omega_m = 0.25$, cosmological constant term, $\Omega_\Lambda = 0.75$, Hubble parameter $h = H_0/$ (100 km s^{-1} Mpc^{-1}) $= 0.73$, power spectrum normalization, $\sigma_8 = 0.9$, and spectral index $n_s = 1$[1].

2 THEORETICAL MODELS

We begin by describing the Aquarius N-body simulations used to build the merger trees employed by the semi-analytic galaxy formation model, GALFORM. We then describe briefly the updates that we have made to GALFORM itself to include physical processes that are relevant on the scale of low mass galaxies.

2.1 The Aquarius halos

In the Aquarius project, carried out by the Virgo Consortium, six galactic dark matter halos with masses comparable to that of the Milky Way were simulated at varying levels of resolution (Springel et al. 2008a,b). Here, we use all six halos at the second highest level of resolution (‘Level 2’ in Springel et al. 2008b)[2]. We define as ‘satellites’ all sub-halos found by SUBFIND (Springel et al. 2001) with more than 20 bound particles. Merger trees were constructed for each subhalo using the methods laid out in Helly et al. (2003) and Harker et al. (2006).

Table 1 provides a summary of the relevant properties of the Aquarius halos, taken from Springel et al. (2008b). The halos all have virial masses in the range 1–$2 \times 10^{12} M_\odot$. Recent evidence from the analysis of Guo et al. (2011a) suggests that the current best estimate of the Milky Way's halo mass is $2 \times 10^{12} M_\odot$, with a 10% to 90% confidence interval spanning the range 0.8 to $4.7 \times 10^{12} M_\odot$; other studies,

---

[1] These parameters were chosen to match the WMAP 1st-year results. Of these, only σ_8 and n_s are of importance for our study. The adopted value of σ_8 leads to an earlier redshift of reionization than expected for the WMAP 7-year value ($\sigma_8 = 0.80$), but this is partly compensated for by the larger value assumed for n_s (0.96 from the WMAP 7-year data). In any case, these differences are expected to be small (?Boylan-Kolchin et al. 2010; Iliev et al. 2011), especially compared with those arising from uncertainties in the modelling of reionization (e.g., the assumed escape fraction or the clumping factor).

[2] The highest level of resolution, ‘Level 1’, is available only for one of the halos.

Halo name	m_p [M$_\odot$]	N_{hr}	$M_{200}[M_\odot]$	r_{200} [kpc]	$M_{*,tot}[M_\odot]$ fbk:sat/rei:G+L ($f_{\rm esc}=1$)
AqA	1.370×10^4	531,570,000	1.842×10^{12}	245.88	1.085×10^{11}
AqB	6.447×10^3	658,815,010	8.194×10^{11}	187.70	9.179×10^9
AqC	1.399×10^4	612,602,795	1.774×10^{12}	242.82	1.050×10^{11}
AqD	1.397×10^4	391,881,102	1.774×10^{12}	242.85	6.982×10^{10}
AqE	9.593×10^3	465,905,916	1.185×10^{12}	212.28	2.217×10^{10}
AqF	6.776×10^3	414,336,000	1.135×10^{12}	209.21	6.555×10^9

Table 1. Properties of the Aquarius halos, as given by Springel et al. (2008b). Listed here are: the particle mass, m_p; the total number of particles in the high resolution region, N_{hr}; the virial mass of the halo, M_{200}; and its virial radius, r_{200}. The last column gives the total stellar mass for each Aquarius halo in the fiducial model, fbk:sat/rei:G+L ($f_{\rm esc}=1$), that will be described later in the paper. The stellar masses in this model show a large scatter around the value estimated for the Milky Way, $4.85-5.5\times10^{10}M_\odot$ by Flynn et al. (2006).

however, favour a mass closer to $10^{12}M_\odot$ (Battaglia et al. 2006a; Smith et al. 2007; Xue et al. 2008). Thus, the Aquarius halos sample the lower end of the currently plausible range of Milky Way halo masses and could underestimate the true mass by a factor of 2–3. This would have important consequences for the properties of subhalos and, therefore, for any satellite galaxies they may contain. We have checked whether the central galaxies in our models have stellar masses comparable to those estimated for the Milky Way, $4.85-5.5\times10^{10}M_\odot$ (Flynn et al. 2006). The final column of Table 1 shows the new fiducial model that will be described later in more detail. The total stellar masses seem realistic, although there is significant variation from halo to halo.

2.2 GALFORM: The basic model

Our starting point is the implementation of GALFORM by Bower et al. (2006). GALFORM includes the treatments, introduced by Cole et al. (2000), of shock-heating, radiative cooling of gas within dark matter halos (modulo the reduction in cooling rates due to photoionization described below), star formation, spheroid formation (through both disk instabilities and galaxy merging), chemical evolution and dust extinction. In addition, this version contains prescriptions introduced by Bower et al. (2006) for feedback from active galactic nuclei (AGN) and supernovae explosions, and mass loss in stellar winds. The Bower et al. (2006) galaxy formation model reproduces properties of the galaxy population over a wide range of scales and epochs. For example, it gives a good match to the global luminosity and stellar mass functions and to the bimodal colour distribution of galaxies observed in the SDSS and can also account for the redshift evolution of these properties.

Font et al. (2008) have found that the relative distribution of SDSS galaxy colours amongst the blue and red sequences, as well as the zero-point of the bimodal colour distribution, can be better matched by GALFORM by setting the metallicity yield to $p=0.04$ (i.e., twice the value adopted by Bower et al. (2006)). In addition, increasing the yield by this factor results in a better match to the metallicity of the intracluster medium (Bower et al. 2008) and improves the predicted metallicities of the dwarf galaxies that are of interest here. For these reasons, we adopt this higher value of the yield in this paper. As in the study of Bower et al. (2006), we assume that the hot gaseous halos of satellites are completely and instantaneously stripped by ram pressure as soon as they cross the virial radius of their host halo. (McCarthy et al. (2008) have shown that ram pressure stripping of hot gas around satellites in groups and clusters can occur on a relatively long timescale but for satellites of galaxies like the Milky Way, the assumption of instantaneous stripping is a good approximation.)

Feedback from supernovae plays an important role in establishing the properties of Milky Way satellites. In this paper, we investigate different feedback schemes and how they affect both the luminosity function and the luminosity - metallicity relation. The first feedback scheme we analyse is the implementation in GALFORM presented in Bower et al. (2006) (hereafter the “default model” or fbk:B06). In the Bower et al. (2006) model, supernovae are assumed to inject energy into the cold gas in the disk of the galaxy, heating it to the virial temperature of the halo after which the gas is ejected. This ‘reheated’ gas may subsequently cool and resettle into the disk. The efficiency of stellar feedback, β, is assumed to depend on the circular velocity of the halo, v_H, in which the galaxy resides as $\beta=(v_H/v_{\rm hot})^{-\alpha_{\rm hot}}$ (see also Cole et al. 2000). The parameters $v_{\rm hot}$ and $\alpha_{\rm hot}$ control the feedback efficiency, and in the Bower et al. (2006) model, they are set to $v_{\rm hot}=485$ km s^{-1} and $\alpha_{\rm hot}=3.2$. Note that larger values of $\alpha_{\rm hot}$ correspond to a greater effectiveness of supernova feedback in halos with $v_H<v_{\rm hot}$, which is the regime of interest here.

As we shall see in Section 3.1, the stellar feedback assumed in Bower et al. (2006) leads to model satellites with metallicities lower than observed. This happens because the supernova feedback in this model is too efficient at expelling metals from dwarf galaxies. We find that simply decreasing the slope of the $\beta(v_H)$ dependence is not a viable solution to this problem: while reasonable matches to the satellite metallicities can be found with, for example, $\alpha_{\rm hot}\simeq2.5$, this approach leads to a boost in the number of field dwarf galaxies which is inconsistent with data from large-scale surveys.

We consider the possibility that supernova feedback may not scale as a simple power law across the full range of galaxy masses and investigate alternative formulations that preserve the good agreement with large-scale data that was the trademark of the Bower et al. (2006) model. In Section 3.2 we find a viable model which has the property that the efficiency of stellar feedback, β, saturates in small mass halos, with $v_{\rm circ}\leqslant65$ km s^{-1}, while above this value it retains the behaviour of the default model. This model is

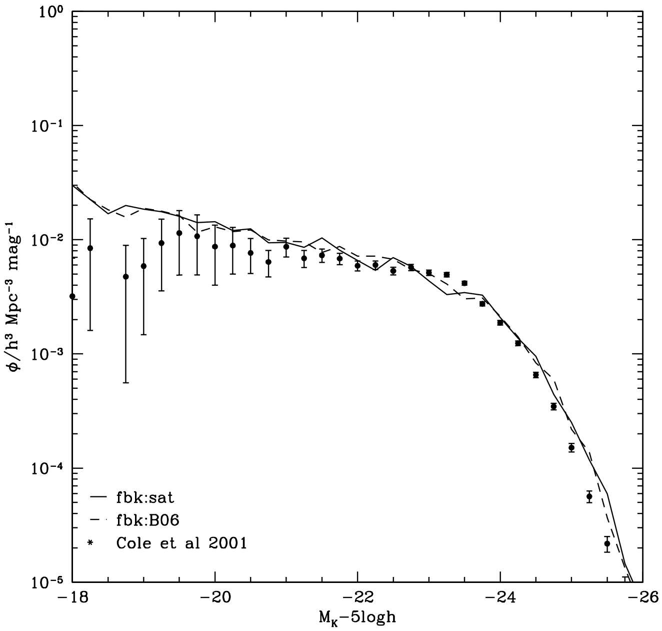

Figure 1. Comparison of the global K-band luminosity function for the fiducial model with saturated feedback used in this paper (full line) and the Bower et al. (2006) model (dashed line). The models are compared with observational data from Cole et al. (2001). Although the two models differ in their treatment of stellar feedback below $v_{\rm circ} = 65$ km s^{-1}, they provide entirely comparable fits to the observational data at brighter magnitudes.

called fbk:sat. It matches the global properties of the galaxy population well (see Fig. 1, for example) and, as we will show below, also a variety of Local Group data, including the flattening of the metallicity-luminosity relation observed for the ultra-faint dwarfs. The stellar feedback is required to be very inefficient in these systems.

It seems plausible that the feedback efficiency is low in small mass galaxies because their star formation rate (and hence the supernova rate) is observed to be low. Dwarf galaxies may be pre-enriched by Population III stars to a level of order $10^{-3} Z_\odot$ (Wise et al. 2010). Afterwards, due to the inefficient feedback, the smallest dwarfs would evolve approximately as a closed-box system (Salvadori & Ferrara 2009), and a single generation of supernovae may be sufficient to increase their metallicity by ~ 0.5 dex, as observed. We note that a similar saturation scheme has been proposed recently by Guo et al. (2011a), who implemented it in the Munich semi-analytic model. Theirs is the first model that successfully matches both the large-scale data and the properties of dwarf galaxies, although only at the resolution of the Millennium-II simulation, $m_p \simeq 9.4 \times 10^6 M_\odot$ (Boylan-Kolchin et al. 2009). Table 2 summarizes the main feedback and reionization features of the models used in the paper.

When modelling galaxy formation in lower resolution simulations than Aquarius care must be taken to follow satellite galaxies in subhalos that are disrupted below the adopted particle limit (20 in our case) by tidal forces. In the terminology of Springel et al. (2001), these galaxies are of 'type 2' while galaxies present in identified dark matter subhalos are of 'type 1'. At the resolution of Aquarius ($\sim 10^4 M_\odot$), we can safely assume that whenever a subhalo is disrupted so is the galaxy (if any) that it contains, that is, there are no type-2 galaxies. Changes in the structure of subhalos caused by baryons cooling inside them are likely to be negligible since satellites have very large mass-to-light ratios. We have checked that the sizes of potential type-2 satellites given by GALFORM (including the effects of adiabatic contraction caused by the bayrons) immediately before their subhalos are disrupted are generally larger than the subhalo tidal radius. We therefore assume that 'type 2' galaxies are disrupted when their halos are disrupted and exclude them from further analysis.

With the exception of the additional physical processes discussed below, all the other parameters in our semi-analytic model are the same as in Bower et al. (2006).

2.3 Additional physics

Here, we briefly describe the inclusion of new physical processes, relevant on dwarf galaxies scales, in the GALFORM model.

2.3.1 Cooling, reionization, and photoheating

The cooling function, $\Lambda(\rho, T, Z, z)$ (which is the net cooling rate of gas, obtained by summing the cooling and heating terms), is calculated self-consistently at each redshift using the photoheating background predicted by our model of the evolution of the intergalactic medium (IGM) as described below. To carry out this calculation we employ the code CLOUDY (Ferland et al. 1998). The radiative cooling processes included are: Compton cooling off the cosmic microwave background, thermal bremsstrahlung, and the usual atomic radiative processes. We also include molecular (H_2) cooling following the prescription of Benson et al. (2006).

Our model for the evolution of the IGM is essentially that described in Benson et al. (2006) (see also Benson & Bower 2010), which follows the photoionization and recombination of the IGM in addition to cooling and heating rates thereby allowing the ionization and thermal state of the IGM to be predicted as a function of time. The photoionizing flux present at any point within an Aquarius halo is made up of two contributions, a local one due to sources within the halo and a global one due to sources in the rest of the Universe. The calculation of the local flux is explained in Section 2.3.2. To obtain the global flux, we run the GALFORM code on a very large set of Monte-Carlo merger trees generated using the empirical modification of the extended Press-Schechter (1974) formalism advocated by Parkinson, Cole & Helly (2008), which gives results consistent with N-body simulations. This method gives the properties of the IGM outside the Aquarius halo, as well as the global photoheating background. At each timestep in the GALFORM calculation, we determine the mean emissivity (as a function of wavelength) per unit volume in the Universe by summing the contributions of galaxies and quasars. This emissivity is used to compute the rate at which the background of ionizing photons is built up. The background can experience absorption by neutral gas in the IGM, and so it is strongly suppressed prior to reionization.

Model name	Supernova feedback efficiency (β)	Global reionization	Local reionization	Escape fraction ($f_{\rm esc}$)
fbk:B06/rei:G	Bower et al. (2006)	✓	×	1
fbk:B06/rei:G+L	Bower et al. (2006)	✓	✓	1
fbk:sat/rei:G	Saturated	✓	×	0.1, 0.2, 0.5, 1
fbk:sat/rei:G+L	Saturated	✓	✓	0.1, 0.2, 0.5, 1

Table 2. Features of the models. The name of each model reflects whether it includes the default supernova feedback (fbk:B06) efficiency of Bower et al. (2006) or the saturated feedback efficiency (fbk:sat), whether it includes global (rei:G) or local (rei:L) reionization. (Details of the reionization model are given in 2.3.)

For galaxies, the emissivity is obtained self-consistently from the population of galaxies formed by GALFORM up to the current timestep. The efficiency with which this radiation ionizes the IGM depends on the assumed escape fraction of ionizing photons. While both observational and theoretical estimates of this fraction exist (e.g. Atek et al. 2009; Laursen et al. 2009; Siana et al. 2007; Wise & Chen 2009), its value remains highly uncertain, particularly at high redshift. We therefore chose to treat the escape fraction as a free parameter which we fix so as to produce a reionization history compatible with experimental constraints (Komatsu et al. 2010). As we will show in Section 3.2, we find that our new model requires a high escape fraction ($\sim 80-100\%$) in order to match the present number of satellite galaxies. The high escape fraction reflects the fact that our model produces too few ionizing photons at high redshifts to reionize the Universe sufficiently early.

The escape fraction in our model is clearly unrealistically large. Observational estimates suggest values of $\lesssim 10-20\%$ (e.g. Siana et al. 2007; Vanzella et al. 2010; but see Bolton & Haehnelt 2007), but we are forced to adopt a value of $\sim$100% to achieve reionization by a sufficiently high redshift. While it is unclear whether the observed values are representative of the galaxy population as a whole (e.g. if unobserved, low luminosity galaxies dominate the production of ionizing photons, and their escape fractions are much larger, then the ionizing emissivity-weighted escape fraction may be much larger), this is nevertheless a point of tension between our model and current empirical expectations.

Other models of the formation of the Local Group satellites have not attempted to model the formation of galaxies and the process of reionization self-consistently as we have here, and so have been able either to choose an epoch of reionization consistent with constraints, or to put in an ionizing emissivity by hand that is designed to give a reasonable epoch of reionization.

For the purposes of this work, which is concerned primarily with the Local Group satellite galaxies, and not with the process of reionization itself, we take the pragmatic view that we should do whatever is necessary to obtain a realistic epoch of reionization since it is this that primarily impacts the formation and suppression of dwarf galaxies. The fact that this requires a large escape fraction is interesting, and deserves further attention, but is not surprising given that both observations and our model are highly uncertain in the high redshift regime. A better model will most likely need to produce more ionizing photons at high redshift thereby allowing the escape fraction to be reduced. Of course, a self-consistent calculation of the escape fraction for model galaxies would provide a more rigorous way to approach this problem (e.g. Fernandez & Shull 2011). A more detailed study of reionization in the GALFORM model is currently underway (see Raicevic et al. 2010) and will explore this issue in greater depth.

For calculating the emissivity of quasars, we use the code CUBA (Haardt & Madau 2001), which includes an updated version of the observationally inferred Haardt & Madau (1996) spectrum. This approach allows us to track the evolution of the IGM while simultaneously calculating the heating rate of the gas inside galaxies.

Heating due to UV photoionization (photoheating, for short) not only offsets cooling losses but it also prevents low mass dark matter halos from accreting their full complement of baryons. The suppression of baryonic accretion into halos is modelled using the accretion mass scale recently derived by Okamoto et al. (2008) (see also Hoeft et al. 2006) from cosmological hydrodynamical simulations. These authors find that the baryon fraction, $f_{\rm b} \equiv M_{\rm b}/M$, depends on halo mass and redshift as:

$$f_{\rm b}(M,z) = \langle f_{\rm b} \rangle \left[1 + (2^{\alpha/3} - 1) \left(\frac{M}{M_{\rm c}(z)} \right)^{-\alpha} \right]^{-3/\alpha}, \qquad (1)$$

where $\langle f_{\rm b} \rangle = \Omega_{\rm b}/\Omega_0$ is the universal baryon fraction, $M_{\rm c}(z)$ is a characteristic mass that will be defined below, and $\alpha = 2$ provides a good fit to the results of the simulations. It is worth noting that the Okamoto et al. (2008) accretion mass scale is significantly lower than the “filtering mass” calculated previously by Gnedin (2000) on the basis of linear perturbation theory. With this new method, halos that accrete only half of the universal baryon fraction (i.e. $f_{\rm b} = \langle f_{\rm b} \rangle /2$) have, on average, circular velocities of about 25 km s^{-1} at redshift $z = 0$, compared with 50 km s^{-1} found by Gnedin (2000). In other words, the Okamoto et al. (2008) mass accretion scale allows more satellites to escape the effects of the reionization than the associated filtering mass in the Gnedin (2000) formalism. (The latter was used in the previous versions of GALFORM). As we will show, this has important consequences for the inferred role of supernova feedback on relatively massive satellites.

We follow the method suggested by Okamoto et al. (2008) for implementing their scheme of baryon accretion, which involves computing the equilibrium temperature of gas as it accretes into the halo, $T_{\rm accr}$. The simple expectation is that the characteristic mass scale should be set such that $T_{\rm vir}(M_{\rm c}[z], z) = T_{\rm accr}(z)$ where $T_{\rm vir}(M)$ is the virial temperature of a halo of mass M at redshift z. However, Okamoto et al. (2008) show that this approach overestimates the suppression mass scale and does not accurately

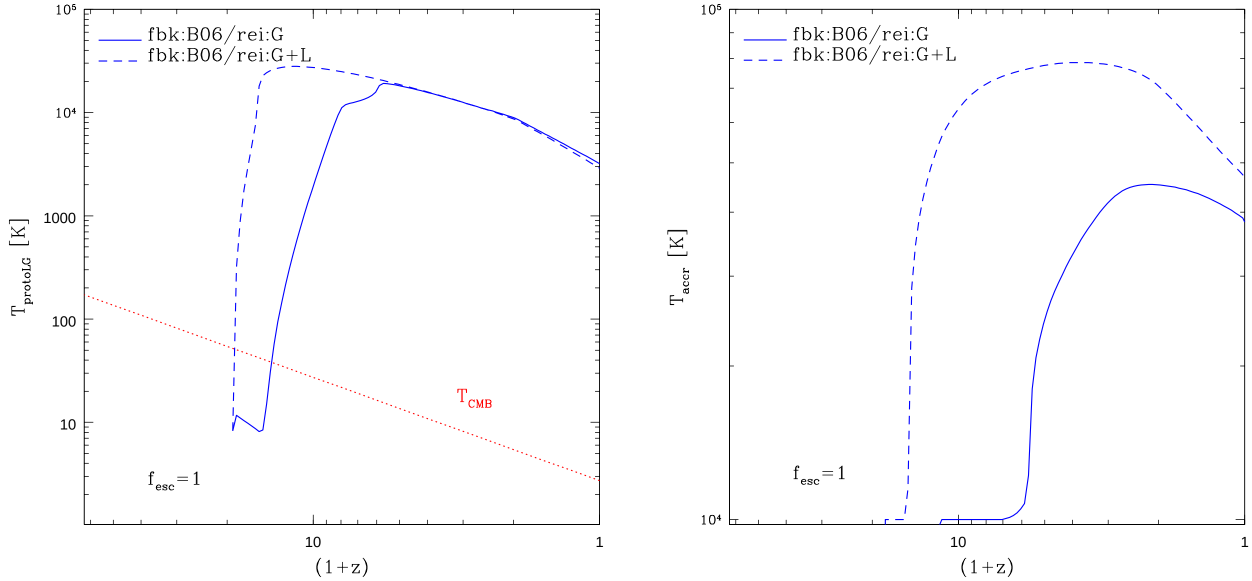

Figure 2. Evolution of the IGM in the default feedback (Bower et al. 2006) model. *Left*: the mean temperature of the gas in the proto-Local Group region in the models with and without the added local UV flux, as a function of redshift (dashed and solid blue curves respectively). Reionization occurs at $z \simeq 14$ in the model with local and global UV flux and at $z \simeq 6$ in the model with only global UV flux. In the first model, the temperature peaks at just below 3×10^4K whereas in the second model it peaks at 2×10^4K. Both models assume an escape fraction of 100%. The temperature of the CMB is shown with a red dotted line for reference. *Right:* the characteristic accretion temperature of gas, $T_{\rm accr}$, as a function of redshift. The accretion temperature peaks at $z \simeq 3$, at a value of 8×10^4K in the model with local UV production, and only at $z \simeq 1.5$, at a value of 4.5×10^4K, in the model with only global UV production. Note the different scales on the y-axis of each panel.

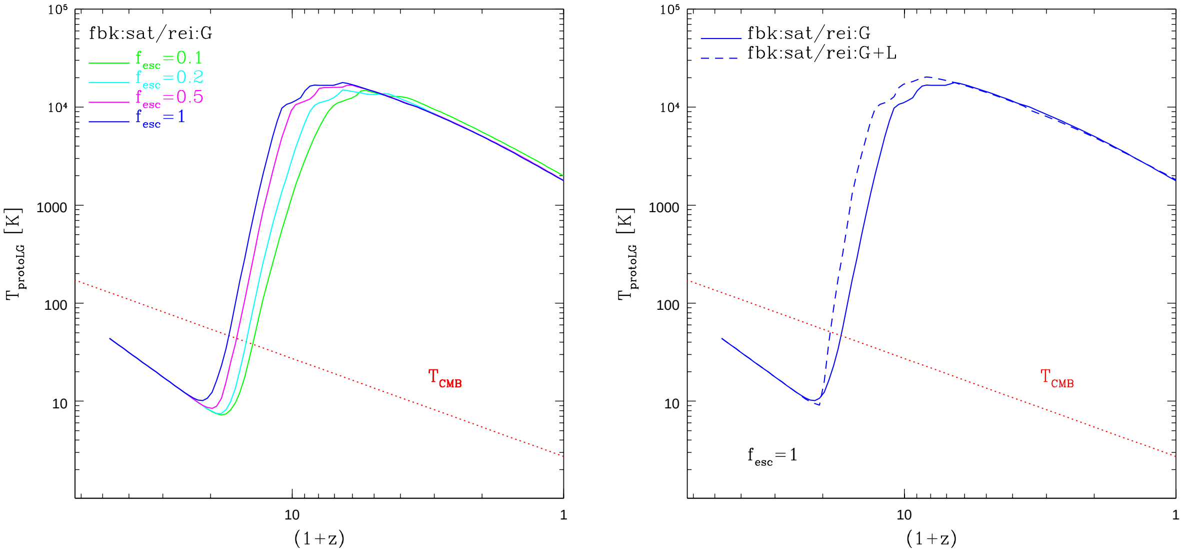

Figure 3. Evolution of the mean temperature of the gas in the proto-Local Group region in the model with saturated feedback. The left panel corresponds to the case of global reionization only, with different colours indicating the escape fraction. Global reionization occurs at $z \simeq 7.8$ for $f_{\rm esc} = 1$, $z \simeq 6$ for $f_{\rm esc} = 0.5$, $z \simeq 5.5$ for $f_{\rm esc} = 0.2$ and $z \simeq 4.5$ for $f_{\rm esc} = 0.1$ respectively. $T_{protoLG}$ peaks at $\sim 2 \times 10^4$K for $f_{\rm esc} = 1$ and decreases slightly to $\sim 1.5 \times 10^4$K for $f_{\rm esc} = 0.1$. The temperature of the CMB is shown with a red dotted line for reference. The right panel shows a comparison of $T_{protoLG}$ in the saturated feedback model with and without local reionization, for $f_{\rm esc} = 1$ (dashed and solid blue lines, respectively). Local emission shifts the redshift of reionization from $z \simeq 7.8$ to $z \simeq 10$, without a significant increase in the peak of the gas temperature.

reproduce the redshift dependence found in their simulations. Instead, they recommend a simple model in which each halo accretes gas at the universal rate (i.e. Ω_b/Ω_0 times its total mass accretion rate) if $T_{\rm vir} > T_{\rm accr}$, and accretes no gas if $T_{\rm vir} < T_{\rm accr}$. We adopt their model in this work. The accretion temperature is computed self-consistently using the cooling function described above and the known density of accreting material. Note that the Okamoto et al. (2008) formalism provides the accretion mass scale only after the epoch of reionization, when there is a significant ionizing background, at which point the authors suggest setting the critical temperature to the equilibrium temperature for the photoionized accreting gas. At earlier times, prior to reionization, we assume that the pre-shock temperature of gas as it is accreted onto a halo is given by the temperature to which it is adiabatically heated up from the mean IGM temperature, or 10^4K, whichever is lower. This is a valid approximation prior to reionization as the IGM gas will be mostly neutral, atomic and metal-free and so there are no efficient cooling processes below 10^4K, and little photoheating due to the lack of a significant ionizing background. At later times, the full complement of heating and cooling processes are used to compute the accretion temperature.

Our treatment of reionization can be compared to other semi-analytic/semi-numerical approaches. In particular, Mesinger, Furlanetto & Cen (2011) recently described a semi-numerical algorithm to compute the ionization state of the IGM. Unlike us, Mesinger, Furlanetto & Cen (2011) compute a position-dependent ionization fraction by recourse to cosmological simulations which they use to estimate densities, collapsed fractions and star formation rates (assuming a constant efficiency to convert collapsed fraction to star formation). In contrast, our model assumes a uniform reionization, but additionally solves for the thermal state of the IGM and has a much more detailed treatment of the underlying galaxy formation physics to predict the ionizing emissivity. Further advances in modelling of reionization must combine aspects of these and other approaches. For example, Raicevic et al. (2010) compute position-dependent reionization by combining a detailed model of galaxy formation with ray-tracing through a cosmological simulation of the density field.

2.3.2 The local UV flux from Milky Way sources

In addition to the global photoionizing flux originating from large scales (from AGN and quasars), *local* sources can also be important contributors, especially at high redshift. If these local sources are significant, reionization in the region will occur earlier than in an average region of the Universe. Thus, the entire region destined to become the Local Group may be encompassed within an ionized bubble ("local reionization"), before many such bubbles have percolated to reionize the Universe as a whole ("global reionization"). One consequence of local reionization is to suppress further the formation of dwarf satellites within the region.

A fully self-consistent treatment of local reionization requires not only accounting for the emissivity of local sources, but also knowledge of other (at the moment, poorly constrained) parameters, such as the photon escape fraction and the gas clumping factor, and modelling of radiative transfer. A comprehensive treatment of this kind has not been performed so far. Current models that do include radiative transfer (e.g. Weinmann et al. 2007; Iliev et al. 2011) have very simplified physical prescriptions for star formation and feedback. Semi-analytical models such as GALFORM, which have more realistic star formation and feedback prescriptions and which match a wide range of observations, by contrast, do not include radiative transfer. The combination of the two approaches is clearly desirable for a complete understanding of the role of local reionization (see Raicevic et al. 2010 for an example of progress in this area). Below we present a simple method for accounting for the local photons. Without radiative transfer, this is likely to overestimate the contribution of local photons to the suppression of low-mass satellites. Nevertheless, we present the results here as proof of concept of how the redshift of reionization is increased by contribution from pre-galactic sources.

To calculate the contribution to the ionizing flux from local sources, we identify the galaxy's progenitors by finding halos in the merger tree that lie within the virial radius of the final Aquarius halo at $z = 0$. We then calculate the total luminosity of ionizing photons emitted by these local sources at all redshifts, and compute the effective photon density within the Lagrangian radius of the final halo:

$$n(z) = \frac{L_{\rm ion}(z)}{4\pi R^2{}_{\rm Lag}(z){\rm c}}\,, \qquad (2)$$

where $L_{\rm ion}(z)$ is the total instantaneous ionizing luminosity, c is the speed of light and $R_{\rm Lag}(z)$ is the radius of a sphere with volume equal to the physical volume that contains a mass equal to the mass of the final halo at each redshift, assuming that the sphere is at the mean density. To account for local emission, this additional emissivity is added to the mean emissivity computed from the global distribution of galaxies. We find that this local emission is the dominant contribution to the net background at early times, particularly prior to reionization when the global background has been unable to build up as a result of the high optical depth in the IGM. At later times, e.g. for $z < 2$, the local contribution becomes entirely negligible. Accounting for the local emission in this way is an approximation that will be valid when the integrated background is dominated by recently emitted light. Prior to reionization, this is certainly the case, as emitted light is rapidly absorbed by neutral gas. Post reionization, the local contribution to the emissivity becomes small compared to the mean global emissivity and so can be neglected.

Fig. 2 shows the evolution of the proto-Local Group region in the default feedback (Bower et al. 2006) model, adopting an escape fraction of ionizing photons of 100%. The left-hand panel illustrates the redshift evolution of the mean gas temperature in the models with and without the local UV flux. At high redshift, the gas cools adiabatically due to the expansion of the Universe. As the first galaxies form, they begin to photoheat the IGM resulting in a rapid rise in temperature at $z \simeq 20$ when the gas temperature soon exceeds that of the CMB by over 2 orders of magnitude. In the model with both global and local photoionization, the proto-Local Group region is reionized at $z \sim 14$. At that point, the gas reaches its maximum temperature of just under 3×10^4K. In the model without the contribution from local sources, reionization occurs significantly later, at $z \sim 6$ (as in the previous calculation of Benson et al. 2002a) and the maximum temperature that the gas attains is only 2×10^4K. After reionization, the temperature of the proto-Local Group gas declines slowly, at a rate controlled by the balance between cooling and continued photoheating.

The right-hand panel of Fig. 2 shows the characteristic accretion temperature of the gas, $T_{\rm accr}$, as a function of redshift (see Okamoto et al. 2008). The accretion temperature rises rapidly at the epoch of reionization as a strong photoheating background builds up, reaching a value of $\sim 8 \times 10^4$K at $z \simeq 3$ in the model with local sources. In the model without local sources, the maximum temperature is approximately half as high, 4.5×10^4K, and this is only reached at $z \simeq 1.5$. At later times, the accretion temperature begins to fall as the photoheating background declines.

The left panel of Fig. 3 shows the evolution of the mean temperature of the proto-Local Group region in the model with saturated feedback and global reionization only, for various assumed escape fractions of ionizing photons. As expected, for a lower escape fraction global reionization occurs later, but the model results in a more plausible reionization history for large values of the escape fraction (see Stark et al. 2010, for a discussion of recent observational data). The earliest redshift of reionization in this case is $z \simeq 7.8$, for $f_{\rm esc} = 1$, and the latest is $z \simeq 4.5$, for $f_{\rm esc} = 0.1$. The peak of $T_{\rm protoLG}$ is similar in the two feedback models (compare the solid blue lines in the left panels of Figs. 2 and 3). For $f_{\rm esc} = 1$, this temperature is $\sim 2 \times 10^4$K. At a fixed escape fraction, global reionization occurs earlier in the model with saturated feedback than in the model with the default feedback of Bower et al. (2006) ($z \simeq 7.8$ compared with $z \simeq 6$ for $f_{\rm esc} = 1$). This is because a weaker feedback efficiency allows dwarf galaxies to become brighter and therefore emit a larger number of ionizing photons.

The right panel of Fig. 3 shows the effect of adding local reionization in the model with saturated feedback. (We illustrate this for $f_{\rm esc} = 1$, but the other cases display a similar behaviour). In this case, local emission shifts the redshift of reionization from $z \simeq 7.8$ to $z \simeq 10$, while the peak of the gas temperature remains roughly the same. Below, we discuss how different feedback and reionization models affect the satellite luminosity function.

3 RESULTS

In this section, we investigate how different feedback processes affect the broad properties of satellite galaxies. We compare our model predictions not only to the observed satellite luminosity function[3], but also to the observed satellite metallicity-luminosity relation. As we shall see, this relation serves to break a degeneracy in the models between the effects of supernova feedback and reionization.

We will compare our model predictions for the luminosity function with data for the Milky Way, based largely on the SDSS DR5 data. For this, we count all satellites in the model within a radius of 280 kpc, the limit to which the tip of the red giant branch can be detected in the SDSS. We compared this luminosity function to the estimate by Koposov et al. (2008) of the expected number of satellites in the Milky Way within this radius, which is well described by a power-law,

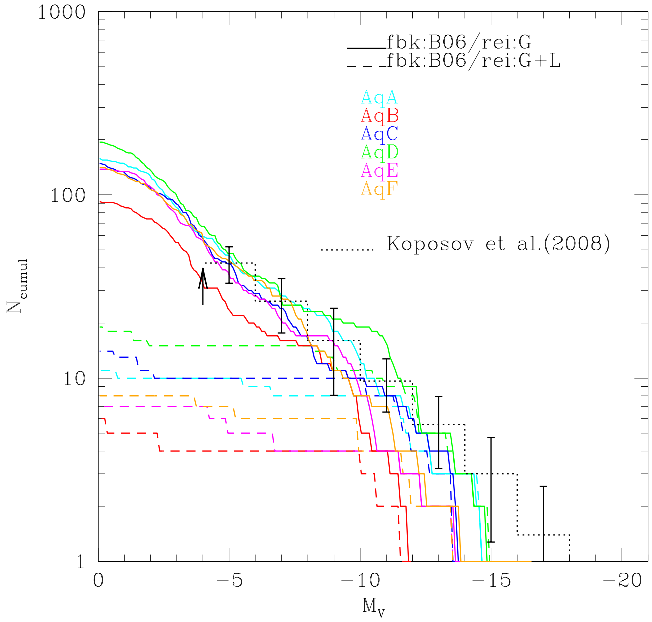

Figure 4. Luminosity functions for the models with default feedback (full lines for global reionization: fbk:B06/rei:G; dashed lines for global plus local reionization: fbk:B06/rei:G+L). The different colours correspond to the six Aquarius halos. The estimate of the Milky Way luminosity function by Koposov et al. (2008) is shown by the stepped dotted line down to the limit of $M_{\rm V} = -5$, below which the volume corrections become very uncertain (this limit is marked in the figure by a vertical arrow). The errorbars are Poissonian for the satellites in the classical ($M_{\rm V} \leqslant -11$) regime, while for the fainter systems they include volume corrections appropriate for the SDSS DR5.

$$dN/dM_{\rm V} = 10 \times 10^{0.1(M_{\rm V}+5)}. \qquad (3)$$

The number of satellites in the Milky Way estimated according to this calculation is shown in the luminosity function plots below by a stepped dotted line. In the "classical dwarfs" regime ($M_{\rm V} \leqslant -11$), the error bars on the observational estimate are assumed to be Poissonian, while in the interval $-11 \leqslant M_{\rm V} \leqslant -5$, additional corrections for the SDSS DR5 volume are included. We do not plot the observational estimates for magnitudes fainter than $M_{\rm V} = -5$ where the volume corrections become very uncertain. Note that in this cumulative plot the errors are not independent. Also note that the above estimate requires an uncertain assumption about the radial distribution of Milky Way satellites (Tollerud et al. 2008).

For properties of the satellite population for which the radial incompleteness of the observational data is important (e.g. the radial distribution of satellites in Section 4.1), we model the incompleteness explicitly within the SDSS DR5 footprint. Firstly, we apply the magnitude dependent threshold of detectability, $R_{max}(M_{\rm V})$, derived by Koposov et al. (2008). Then we randomly select 20% of the satellites to account for the SDSS DR5 partial coverage of the sky. The

---

[3] Unless stated otherwise, we use the term 'luminosity function' to refer to the luminosity function of dwarf satellite galaxies around galaxies like the Milky Way.

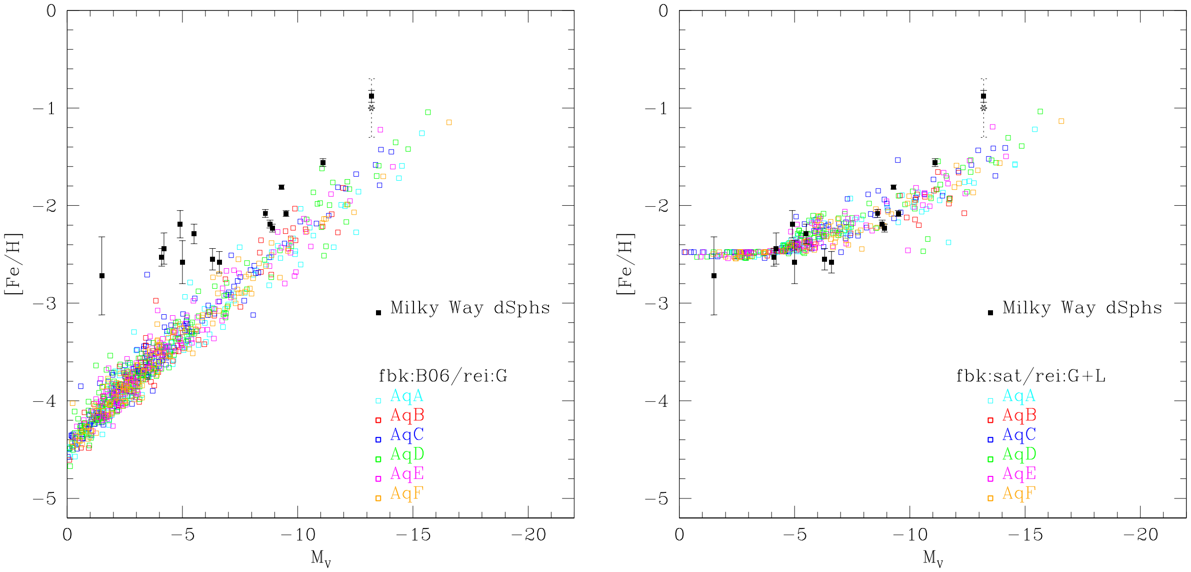

Figure 5. The $Z - M_{\rm V}$ relation for the fbk:B06/rei:G models (*left*) and for the fbk:sat/rei:G+L models (*right*), where Z is the average [Fe/H]. Both models assume $f_{\rm esc} = 1$. The different colours correspond to satellites in the six Aquarius halos. The black squares show the observational data for the Milky Way dwarf spheroidals (Norris et al. 2010). This study includes data for both classical dwarfs (Mateo 1998; Helmi et al. 2006) and ultra-faint dwarfs (Kirby et al. 2008; Martin, de Jong & Rix 2008; Norris et al. 2010), but only for those systems with chemically unbiased star samples. The [Fe/H] error bars have been re-calculated by Norris et al. (2010) using the precepts of Da Costa et al. 1977 (§ III). The star symbol shows the peak of the metallicity distribution function in Fornax measured by Battaglia et al. (2006b) and Kirby et al. (2010) using a larger sample of stars but with lower resolution spectra than Norris et al. (2010). The lower resolution samples cover a larger spatial extent in Fornax and therefore may give a more accurate representation of the average [Fe/H] by taking into account the contribution of metal-poor populations preferentially located at the outskirts (Battaglia et al. 2006b; Letarte et al. 2010).

model "classical" satellites ($M_{\rm V} \leqslant -11$) are all included, under the assumption that they are not affected by incompleteness.

3.1 The default feedback model (fbk:B06)

The combined effects of supernova feedback and reionization in the default feedback model, applied to the six Aquarius halos, are shown in Fig. 4. Models with global reionization only are labelled fbk:B06/rei:G (solid lines) and models which, in addition, include local reionization are labelled fbk:B06/rei:G+L (dashed lines).

Within the scatter, the fbk:B06/rei:G models give a reasonable match to the luminosity function. However, none of the halos host galaxies as bright as the the SMC and the LMC. A similar result was obtained by Benson et al. (2002b), who found that only about 1 in 20 of their Milky Way-type galaxies had satellites as bright as the SMC and the LMC. Remarkably, this result now appears consistent with recent measurements of the prevalence of bright satellites in external galaxies similar to the Milky Way which indicate that only 11% of such hosts have one and 3.5% two satellites as bright as the Magellanic Clouds (Liu et al. 2011). Note that there is a large variation in the number of model satellites from one halo to another: the predicted satellite abundance varies by a factor of about 2, reflecting the different formation histories of the halos. This relatively large scatter highlights the danger of arriving at far-reaching conclusions regarding cosmology based on the single example of the Milky Way. Indeed, Guo et al. (2011b) have recently shown, using SDSS data, that, in the mean, isolated primaries of comparable luminosity to the Milky Way contain about a factor of two fewer satellites brighter than $M_V = -14$ than the Milky Way itself.

In the models, there is a degeneracy between the effects of supernovae feedback and reionization: both suppress galaxy formation in small halos. The metallicity, Z, of the stars and gas in a galaxy that is already assembled is not affected by photoheating. It can, however, be strongly affected by supernova feedback which reduces the effective yield as a consequence of outflows. Thus, the $Z - M_{\rm V}$ relation has the potential to break this degeneracy.

The $Z - M_{\rm V}$ relation in the fbk:B06/rei:G model is shown in the left panel of Fig. 5, for all six Aquarius halos, and compared with observations of Milky Way dwarfs with reliable metallicity measurements (Norris et al. 2010). The default feedback model undershoots the metallicities of dwarf galaxies, particularly for the less luminous systems. (Note that the model already includes the large yield, $p = 0.04$, favoured by Font et al. (2008)). The scatter in the $Z - M_{\rm V}$ relation for all six Aquarius systems is relatively small, suggesting that the merger history plays only a secondary role in determining the slope or zero-point of the relation. We conclude that the supernova feedback in this model is too efficient at expelling metals from dwarf galaxies. We now analyze the saturated feedback model.

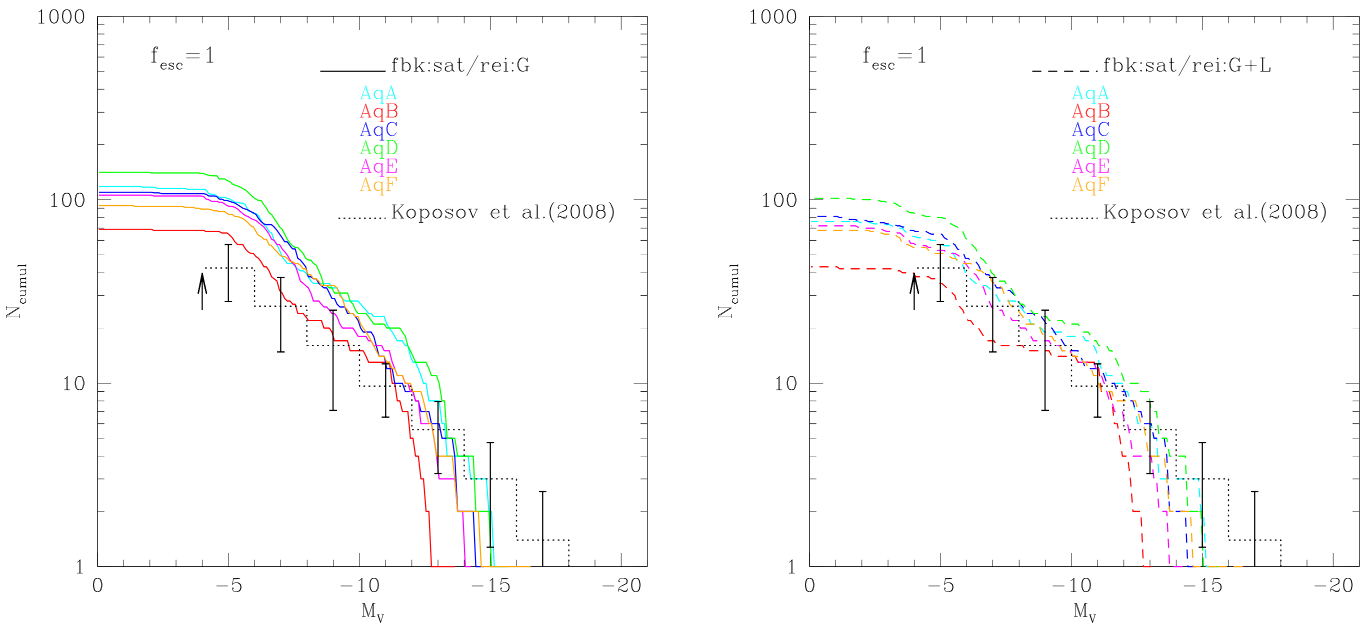

Figure 6. Satellite luminosity functions in the fbk:sat/rei:G and fbk:sat/rei:G+L models for the six Aquarius halos. The photon escape fraction is taken to be $f_{\rm esc} = 1$. The solid lines represent the models with global reionization only and the dashed lines the models with both local and global reionization; different lines correspond to the six Aquarius halos. The observational estimate of Koposov et al. (2008) is shown as a stepped dotted line, as in Fig. 4.

3.2 The saturated feedback model (fbk:sat)

The right panel of Fig. 5 shows the $Z - M_{\rm V}$ relation in the model fbk:sat/rei:G+L. With this feedback prescription, the match to the observed $Z - M_{\rm V}$ relation is greatly improved, especially for the fainter satellites. In particular, the turnover in satellite metallicities is well reproduced. As discussed in Section 2.2, a floor in the average metallicity of satellites can be created by a very inefficient supernova feedback[4]. There are two main regimes in the evolution of dwarf galaxies with inefficient feedback. At early times, there is a significant gas inflow that sustains star formation and an increase metallicity up to $\sim\ 10^{-2.5} Z_{\odot}$ (a single generation of supernovae may be sufficient to increase the gas metallicity by ~ 0.5 dex). This regime is short for the smaller dwarf galaxies, as their gas inflow drops quickly. From then on, the rate of change in metals becomes directly proportional with the outflow which, assuming a constant feedback efficiency, leads to a floor in metallicity.

At the brightest end (i.e., Fornax) our model predicts average metallicities that are below the data point of Norris et al. (2010). However, this measurement is likely to be an overestimate of the actual value because the sample used preferentially contains stars close to the centre of the galaxy (which have higher resolution spectra), and here the stars are more metal-rich (Letarte et al. 2010). Our data are in better agreement with the average Z values inferred from lower resolution spectra that cover a larger extent of this dwarf galaxy (Battaglia et al. 2006b; Kirby et al. 2010).

Fig. 6 shows the luminosity functions of the six Aquarius halos in the fbk:sat/rei:G and fbk:sat/rei:G+L models, for an assumed photon escape fraction of $f_{\rm esc} = 1$. This high value is required to match the observed luminosity function. As mentioned earlier, this value produces a plausible reionization history, but seems higher than indicated by some observational data. Although the escape fraction remains uncertain, such high values (which arise in GALFORM because too few ionizing photons are produced at high redshifts) is probably a shortcoming of the model and requires further investigation. However, for our purposes here, the actual value of the escape fraction is not in itself important. What matters is that there should be enough ionizing radiation to suppress the formation of small galaxies.

Fig. 6 indicates that, unlike in the fbk:B06 case, global reionization alone does not suppress galaxy formation enough in the fbk:sat model to account for the satellite luminosity function. In this case, reionization by local sources is also required. There are important differences in our two feedback models. In particular, the saturated feedback model produces more satellites of all luminosities, even with $f_{\rm esc} = 1$, than the default Bower et al. (2006) feedback model (compare Figs. 4 and 6.) This is largely because the lower feedback efficiency in the saturated model allows galaxies to grow brighter.

In summary, we have found that the model fbk:sat/rei:G+L matches both the global luminosity function (of all galaxies; see Fig. 1), the local luminosity function of Milky Way satellites (see Fig. 6) and the $Z - M_{\rm V}$ relation (see Fig. 5). This model also produces

---

[4] We could not reproduce this flattening of Z at faint $M_{\rm V}$ with a typical power-law supernova feedback, regardless of the change in slope or zero-point.

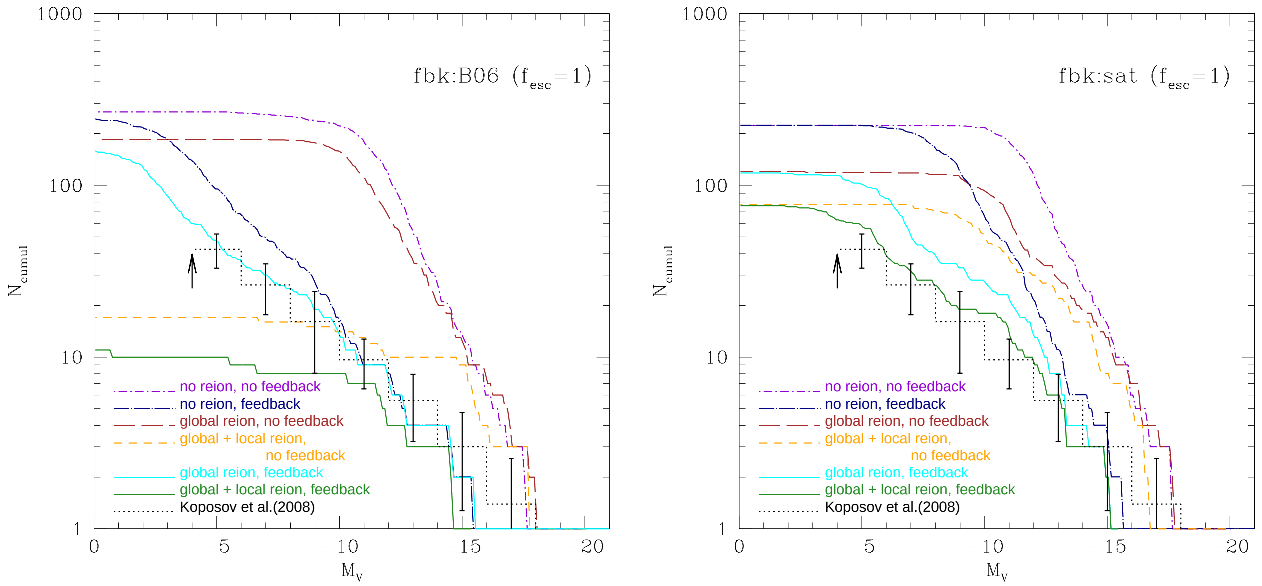

Figure 7. The effect of different physical processes on the luminosity function of satellites in the Aq-A halo, in the models fbk:B06 (*left*) and fbk:sat (*right*). Both models shown here have $f_{\rm esc} = 1$. The purple short-long dashed line shows a model without any reionization or supernova feedback. The dark blue dot-long dashed line shows a model with supernova feedback only, no reionization. The two pure dashed lines show models without supernova feedback but with reionization, dark red long dashes for global reionization only and orange short dashes for global plus local reionization. The cyan full line shows the model with global reionization and feedback. The model with global plus local reionization and supernova feedback is shown with full dark green lines. The observational data and their errorbars are as in Fig. 4.

central galaxy stellar masses roughly consistent with the measured stellar mass of the Milky Way (see Table 1). In Section 4 we will adopt this as the fiducial model and show that it also matches other properties of the Milky Way dwarf satellites.

3.3 The effects of supernova feedback and reionization

Before exploring our fiducial model further, it is instructive to compare the separate effects of the two sources of feedback, supernova energy and reionization, on the satellite luminosity function in the two cases, fbk:B06 and fbk:sat. These are illustrated in the two panels of Fig. 7.

In the absence of feedback of any kind, the purple dot-dashed lines show that in both cases hundreds of satellite galaxies form with V-magnitudes brighter than $M_{\rm V} = -10$. The lack of feedback enables galaxies to retain their baryons and continue to grow in size and luminosity. Below $M_{\rm V} \approx -10$, the cumulative luminosity function levels off due to the inability of gas in halos with virial temperatures below 10^4K to cool efficiently. The effect of reionization by a global UV background (dark red long dashed lines) is not enough, on its own, to lower the number of satellites sufficiently so as to match the observed luminosity function. The effect is minimal in the fbk:B06 model, where it suppresses the formation of satellites only by about 50%. In the fbk:sat model it reduces the number of luminous satellites by a factor of 2, but still overpredicts the bright end. Our model of reionization is based on the hydrodynamic simulations of Okamoto et al. (2008) in which the effects are relatively mild, with gas accretion being suppressed only in halos with circular velocity lower than $\sim$ 25 km s^{-1}. Most previous studies of satellite galaxies have assumed the more aggressive reionization model of Gnedin (2000) in which suppression occurs in halos with circular velocity up to $\sim$ 50 km s^{-1}. However, even in this case, the effects of global reionization are relatively mild (see e.g. Benson et al. 2002b).

The inclusion of local sources of reionization (orange short dashed lines in Fig. 7) has a dramatic effect in fbk:B06, but a relatively weaker effect in the fbk:sat model. This is to be expected since in the fbk:sat model a larger fraction of ionizing emission arises from lower mass progenitors. In the overdense region corresponding to the proto-Local Group these low mass progenitors are less overabundant (relative to their mean abundance averaged over all space) than are more massive progenitors (Mo & White 1996). Thus, the enhancement in the total ionizing emissivity is similarly reduced when accounting for their local contribution. In both cases reionization is pushed back locally to an earlier redshift and galaxy formation is inhibited in halos with very low velocity dispersion. The bright end, $M_{\rm V} < -15$, remains unaffected.

Perhaps the most illuminating is the effect changing the supernova feedback. In the fbk:B06 model this process affects galaxies in halos of all circular velocities. The efficiency is high and supernova feedback dominates global reionization across the entire range of satellite galaxies. In the fbk:sat model, this process becomes scale-dependent. Interestingly, the scale on which supernova feedback saturates, $M_{\rm V} \approx -10$, it is also where it becomes less efficient than global reionization in suppressing the formation of satel-

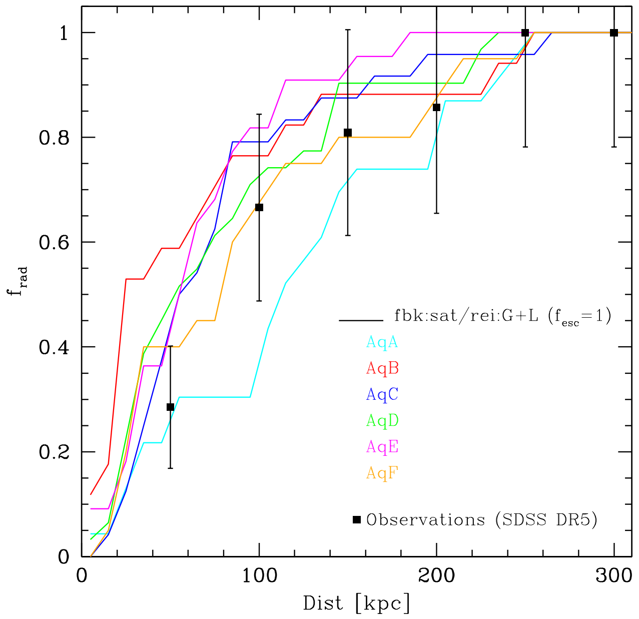

Figure 8. Radial distribution of satellites in the fiducial fbk:sat/rei:G+L model. The observations include both the 11 classical satellites and those detected in SDSS DR5 (compiled from Mateo (1998) and Koposov et al. (2009)), for which the SDSS DR5 threshold selection and sky coverage has been assumed (see text for details). The error bars illustrate the uncertainty due to Poisson statistics. Note that in this cumulative plot the errors are not independent.

lites. Feedback alone (shown by dark blue dot-dashed lines) cannot explain the luminosity function in either model: the abundance of galaxies overshoots the data by a factor of $\sim$ 2 in the fbk:B06 case and by a factor of $\sim$ 10 in the fbk:sat case. In both cases, supernova feedback is the dominant source of suppression of massive, bright satellites (with $M_V < -10$). As found in earlier studies, a combination of feedback and photoheating (global only in fbk:B06 and global + local in fbk:sat) is required to account for the abundance of low-mass satellites.

4 TESTS OF THE FIDUCIAL MODEL

We have selected the parameters of the fiducial model (fbk:sat/rei:G+L) on the basis of the luminosity function and $Z - M_V$ of Milky Way satellites. In this section, we test the model against measurements of the radial distribution of satellites and the relation between the central mass density and luminosity. It is important to note that the model has not been adjusted during this comparison.

4.1 The radial distribution of satellites

Fig. 8 shows the radial distribution of the satellites that survive to the present day in the fiducial model for the six Aquarius halos. As outlined in Section 3, for magnitudes fainter than the classical dwarf regime ($M_V \geqslant -11$), we select only those satellites that could have been observed in the SDSS DR5 survey. The detection of brighter satellites is assumed to be complete and so these are all included. Satellite distances and their uncertainties (typically 10-20%) are taken from Mateo (1998) in the case of the classical dwarfs and from Koposov et al. (2009) in the case of the ultra-faint dwarfs detected in the SDSS DR5.

Overall, the new model displays a radial distribution of surviving satellites similar to the observations (which have large uncertainties). The predicted distributions appear slightly more concentrated than the data for 4 of the 6 halos, less concentrated than the data for one and very close to the data for the remaining halo.

4.2 The $M_{300} - L$ relation

Dwarf galaxies are inefficient retainers of baryons and, as a result, are strongly dark matter dominated. This makes them ideal probes of the dark matter. In particular, their very central regions could contain information about its identity (e.g. Navarro, Frenk & White 1996). Rough estimates suggest a mass of about 10^7 $M_\odot$ within the visible parts of the Milky Way satellite (Mateo 1998; Gilmore et al. 2007). More robust analyses give total masses of about 3×10^9 $M_\odot$ (Wolf et al. 2010; Walker et al. 2010), and, surprisingly, a common mass contained within the central 300 pc, $M_{300} \sim 10^7$ $M_\odot$, independently of luminosity over four orders of magnitude (Strigari et al. 2008).

The high numerical resolution of the Aquarius halos allows us to calculate M_{300} directly from the simulations and, in conjunction with our modelling of galaxy formation in subhalos, to determine how it varies with satellite luminosity. Fig. 9 shows the $M_{300} - L$ relation for the satellite galaxies in the six simulated Aquarius halos, in the case of the fiducial model. We compute M_{300} directly from the simulations, by summing the masses of all particles within 300 pc of the centre of each subhalo.

Since 300 pc is close to the resolution limit of the Aquarius simulations (Springel et al. 2008b), we have checked the numerical convergence of M_{300} using halo Aq-A, for which a higher resolution simulation, at level 1, is available. We created catalogues of subhalos matched in the level 1 and level 2 simulations by pairing up halos according to position, velocity and mass. We find an extremely good correlation between M_{300} for the most massive subhalos at the two levels of resolution, with more scatter present at lower masses, as expected. However, we find that the level 2 subhalos systematically underestimate M_{300} relative to level 1 by about 20%, even in the most massive systems. This difference is sufficiently small that it will not affect our conclusions, but should be kept in mind when comparing model predictions with data. In the following, we present only the level 2 simulations.

Fig. 9 shows that there is broad consistency in M_{300} between the Aquarius simulations and the data of Strigari et al. (2008). However, the masses in the simulations have larger scatter and, in some cases, slightly larger values than the observations. In all cases the simulations show a weak trend with luminosity that is not apparent in the data. The gasdynamic simulations of galaxy formation in Aquarius halo D by Okamoto & Frenk (2009) show a similar trend between M_{600} and luminosity.

In some of our models, a population of very faint satel-

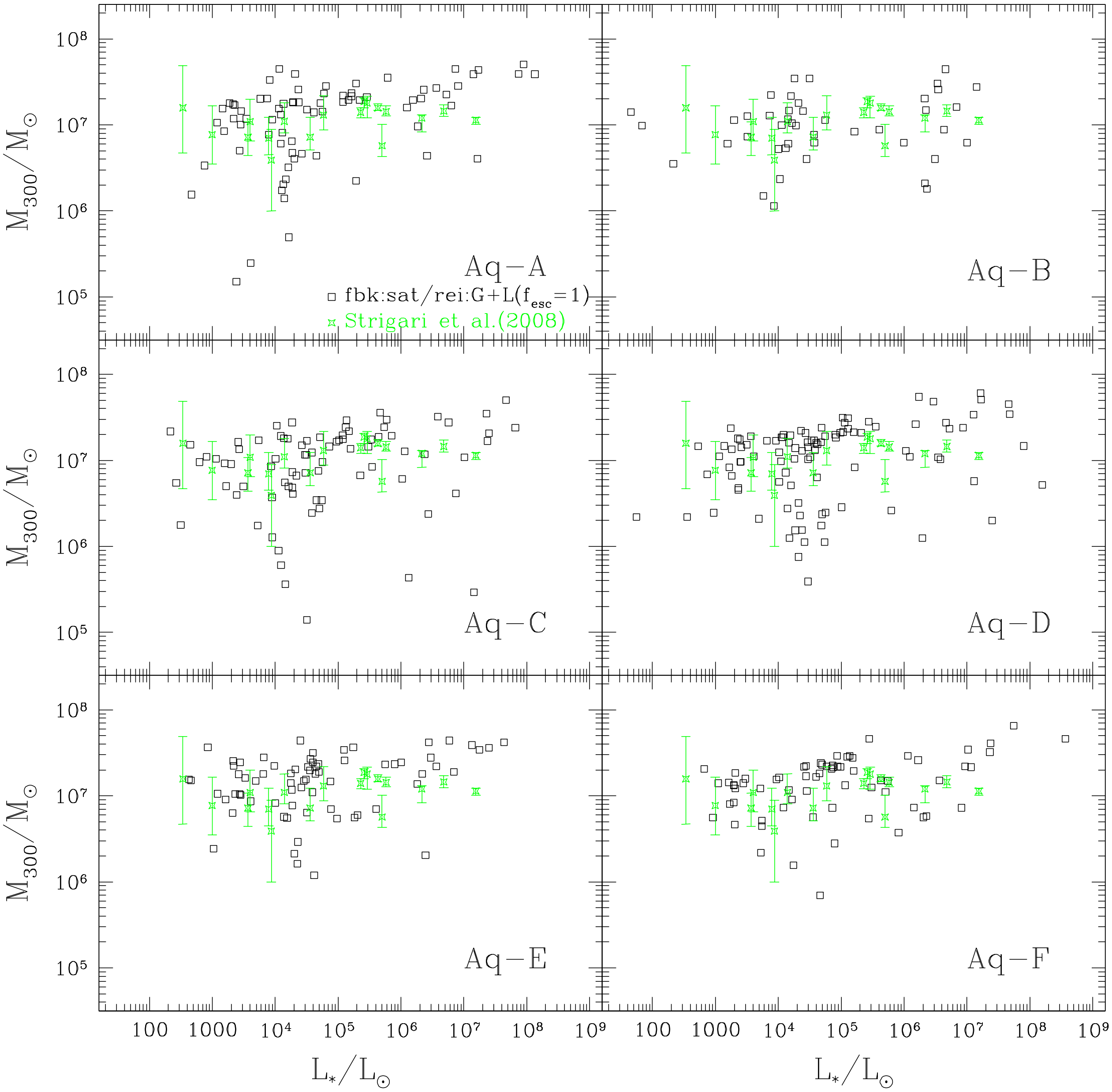

Figure 9. The $M_{300} - L$ relation for satellites in the six Aquarius halos. Results for the fiducial model are shown as empty squares. Observational estimates of M_{300} (green stars) are from Strigari et al. (2008).

lites forms which have values of M_{300} lower than the typical $\sim 10^7$ $M_\odot$ estimated for the real satellites. It may be that systems like this exist in nature but have not been detected so far because of their intrinsically faint luminosities and low surface brightnesses. At the bright end the simulations show a large scatter in M_{300} above and below $10^7 M_\odot$. Better observational statistics may help understand the reason for this discrepancy.

The physical origin of the $M_{300} - L$ relation has recently been discussed by Stringer et al. (2010). We explore this question here by examining the dependence of M_{300} on satellite virial mass.

4.3 The $M_{300} - M_{\rm vir}$ relation

In Fig. 10 we plot the $M_{300} - M_{\rm vir}$ relation for satellites in the six Aquarius halos. Here, $M_{\rm vir}$ is the virial mass before infall into the main halo. The solid line in each panel shows the $M_{300} - M_{\rm vir}$ relation derived for dark matter halos with NFW density profiles (Navarro, Frenk & White 1996, 1997), assuming the best-fit average mass – concentration

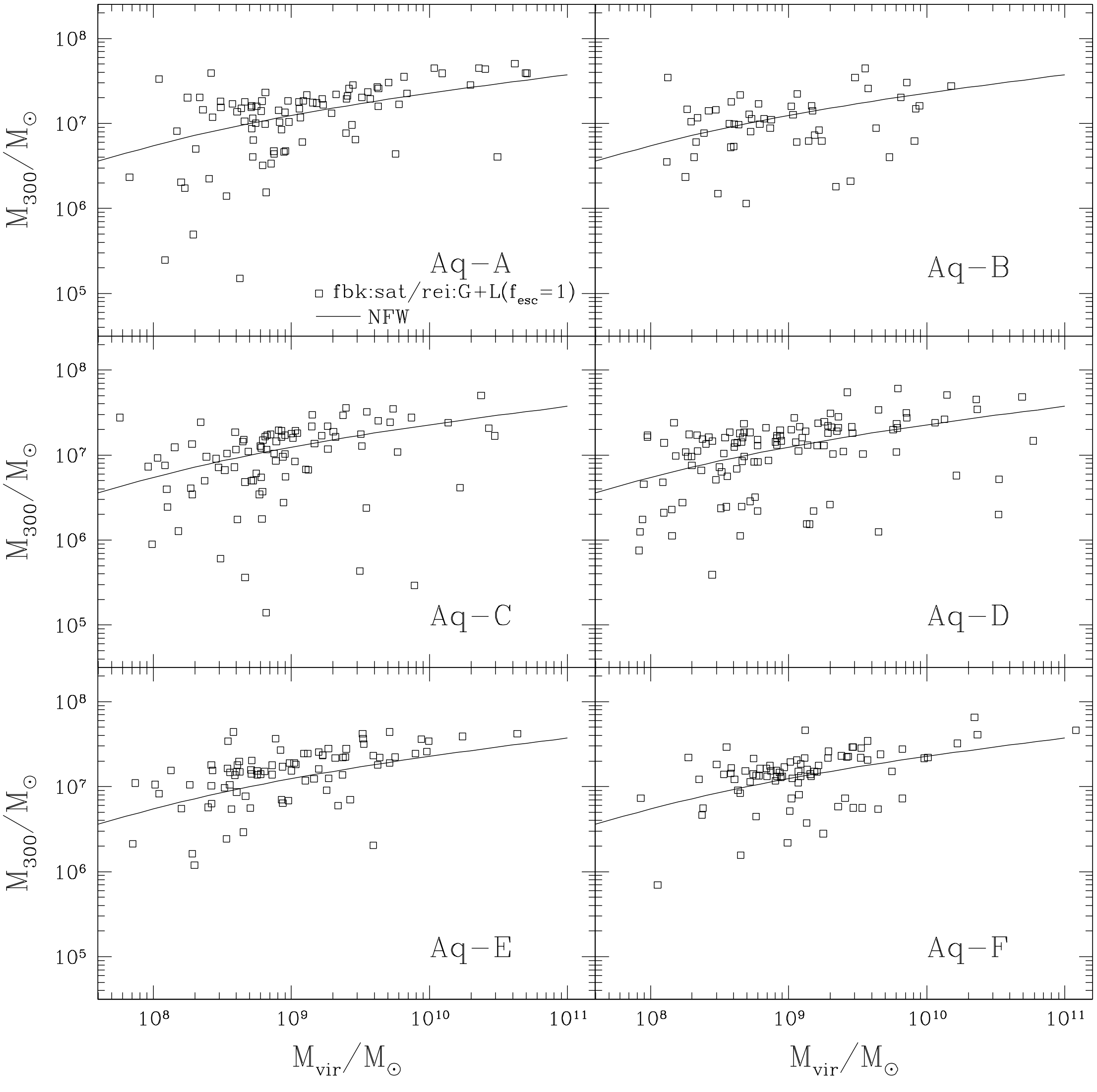

Figure 10. The $M_{300} - M_{\rm vir}$ relation for satellites in the six Aquarius halos. Results for the fiducial model are shown as empty squares. The solid line in each panel shows the $M_{300} - M_{\rm vir}$ relation determined from the Navarro, Frenk & White (1997) dark matter profile, using the mean mass − concentration relation found by Neto et al. (2007).

relation found by Neto et al. (2007). The $M_{300} - M_{\rm vir}$ relation has a similar shape to the $M_{300} - L$ relation, that is, M_{300} depends only weakly on halo virial mass. A power-law fit to the trend yields $M_{300} \propto M_{\rm vir}^{1/3}$. This result can be understood as follows. For a halo of mass $M_{\rm vir} = 10^9 M_\odot$ in the ΛCDM cosmology, the ratio of 300 pc to $r_{\rm vir}$ is ≈ 0.015 and scales as

$$\frac{r_{300}}{r_{\rm vir}} \approx 0.015 \left(\frac{M_{\rm vir}}{10^9 M_\odot} \right)^{-1/3}. \qquad (4)$$

At small radii (in the limit of $r \ll r_{\rm s}$, where $r_{\rm s}$ is the NFW scale radius; Navarro, Frenk & White 1997) in a given halo, the NFW density profile asymptotes to $\rho \propto r^{-1}$, implying a mass profile $M(< r) \propto r^2$. Since the radius r_{300} is much smaller than $r_{\rm s}$ for the halo masses under consideration, the ratio $M_{300}/M_{\rm vir}$ scales as $(r_{300}/r_{\rm vir})^2$. Substituting in the scaling for $r_{300}/r_{\rm vir}$ in equation (4) yields the scaling $M_{300} \propto M_{\rm vir}^{1/3}$ found in the Aquarius simulations.

The weak trend in the M_{300}–$M_{\rm vir}$ relation is the underlying cause of the weak trend in the M_{300}–L relation and

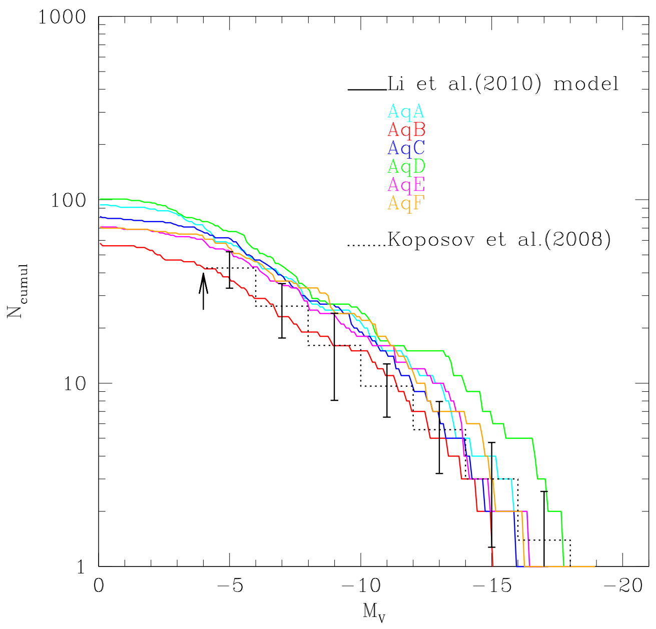

Figure 11. Luminosity functions for the six Aquarius halos in the Li et al. (2010) model.

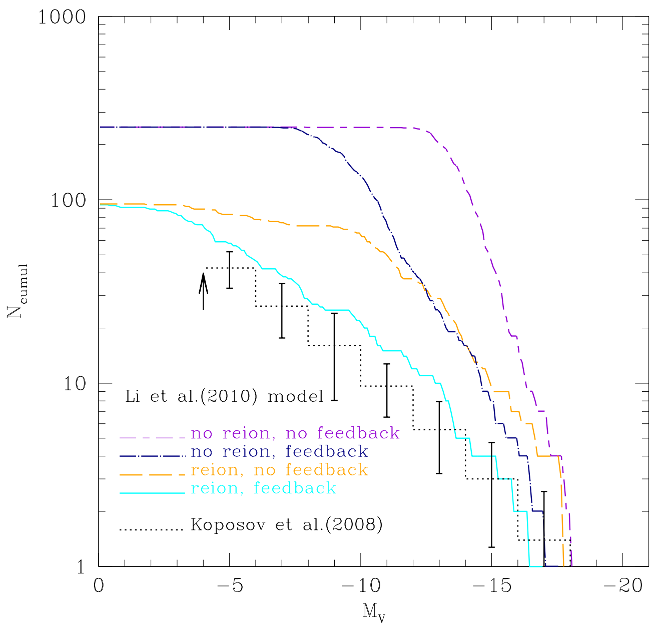

Figure 12. Luminosity function for the Aq-A halo in the Li et al. (2010) model with global reionization and feedback switched on and off.

appears to be a robust prediction of cold dark matter theory unless baryonic processes in the forming dwarf galaxy are able to modify the inner regions of the dark matter density profile significantly.

4.4 A parameterization of the $M_{300} - L$ relation

Summing up the results above, we can now understand why M_{300} appears to be independent of L, even if in reality it has some weak dependence. According to our results, L varies as ${M_{\rm vir}}^n$, where $n \sim 2.5$, and M_{300} varies as $M_{\rm vir}^{1/3}$. This yields the very weak dependence, $M_{300} \sim L^{\beta}$, where $\beta \sim 0.1$, consistent with current observations. This trend is a robust prediction of our models which may, in principle, be tested by further photometric and spectroscopic observations of the faint satellites of the Local Group.

Other theoretical studies find it similarly difficult to reproduce the completely flat $M_{300} - L$ relation seen in the data (Koposov et al. 2009; Macciò et al. 2009; Li et al. 2009; Muñoz et al. 2009; Okamoto & Frenk 2009; Busha et al. 2010; Stringer et al. 2010). In particular, Muñoz et al. (2009) find a similar fit to ours ($M_{300} \sim L^{0.22}$) using the M_{300} values derived from their simulation.

4.5 Comparison with the Li et al. (2010) model

It is instructive to test the robustness of our model by comparing with the results of an independent semi-analytic model implemented in the same six Aquarius halos. This is the "Munich model" described by De Lucia & Blaizot (2007) and applied to galactic satellites by Li et al. (2010). The De Lucia & Blaizot (2007) model reproduces a variety of observational data in the local Universe and at high redshift and, as De Lucia & Helmi (2008) have shown, with some modifications in the treatment of disc instabilities and star formation, it reproduces many observed physical properties of our own Galaxy, including the age and metallicity distribution of stars in its different components. (The modifications of De Lucia & Helmi (2008) do not alter the agreement with observations shown in De Lucia & Blaizot (2007)). Additional updates of the reionization and feedback prescriptions were introduced by Li et al. (2010) to provide a better match to the observed properties of Milky Way satellites. A brief description of the relevant aspects of this model is as follows:

- The cooling model used by Li et al. (2010) is that originally proposed by White & Frenk (1991) and used in subsequent versions of the 'Munich model'. Specifically, the cooling rate depends on the temperature and metallicity of the hot gas, and is regulated by the infall rate in the 'rapid accretion regime'. A comparison between this cooling model and that adopted by Bower et al. (2006) is discussed in De Lucia et al. (2010). Cooling via molecular hydrogen is not included, under the assumption that H_2 is efficiently photodissociated.

- The reionization is modelled using the methodology of Croton et al. (2006), who adopted the Gnedin (2000) formalism. In the Li et al. (2010) model, however, the reionization is assumed to start at redshift $z_0 = 15$ and end at $z_r = 11.5$, that is, earlier than implied by the calculation of Gnedin (2000), who obtained $z_0 = 8$ and $z_r = 7$. The reionization scheme assumed in Li et al. (2010) does not take into account the local photoionization. However, with the final choice of parameters, this model becomes similar to our preferred GALFORM model, fbk:sat/rei:G+L, which includes both global and local reionization and which reionizes completely at $z \approx 10$.

- Supernova feedback is modelled as in De Lucia, Kauffmann & White (2004). With the adopted parameters, galaxies with virial velocity $V_{vir} < 87$ km s^{-1} have more heated gas mass per unit stellar mass than in the standard Croton et al. (2006) and De Lucia & Blaizot (2007) models. Their feedback becomes inefficient for low mass galaxies, similar to the situation in our fbk:sat model (compare the blue dot-long dashed lines in Fig. 12 and in the right panel of Fig. 7).

Li et al. (2010) applied this 'ejection' model to a series of high (but much lower than in Aquarius) resolution simulations of Milky Way-type halos. They found a good match to a variety of observations, including the satellite luminosity function, the luminosity-metallicity relation, the radial and size distributions, and the central mass - luminosity relation. The Li et al. (2010) model yields somewhat higher metallicities than GALFORM for systems with $L_V \gtrsim 10^6 L_\odot$ (but is able to reproduce the metallicities of the ultra-faint satellites).

We apply here the Li et al. (2010) model to the six Aquarius halos analyzed in this study. Fig. 11 shows the satellite luminosity functions, constructed in the same way as for GALFORM (see details in Section 3). Within the scatter there is a reasonably good agreement with the observational estimates of Koposov et al. (2008).

Fig. 12 shows the role of supernova feedback and reionization separately and is similar to Fig. 7 in the case of the GALFORM models. There are several common characteristics between this model and our fiducial model GALFORM model, fbk:sat/rei:G+L: firstly, feedback from supernovae is more effective at suppressing the formation of the more luminous systems, while reionization acts more effectively at the faint end ($M_{\rm V} \geqslant -10$); secondly, the reionization alone does not suppress galaxy formation sufficiently for the model to match the observed luminosity function. (This is reminiscent of the conclusions of Benson et al. (2002b) who also found that global reionization implemented using the Gnedin (2000) formalism has a relatively mild effect).

The comparison between different semi-analytical models highlights the existence of degeneracies in the way in which different physical processes – supernova feedback and reionization, in this case – affect the properties of the resulting galaxies. However, as we have shown, it is often possible to break these degeneracies by comparing the model predictions to a variety of observables rather than to a single property such as the satellite luminosity function.

5 DISCUSSION AND CONCLUSIONS

We have implemented a detailed treatment of reionization in the Durham semi-analytic model of galaxy formation, GALFORM, and applied it to the 6 high-resolution simulations of galactic halos of the Aquarius project. The UV flux produced by the galaxy population is calculated in a self-consistent way and the contribution from quasars is taken from the observationally inferred spectrum of Haardt & Madau (1996). The UV flux inhibits star formation by: (i) preventing gas accretion onto low mass halos, and (ii) offsetting the cooling rate of the gas already inside halos. These effects influence how galaxies form and evolve and this, in turn, affects the strength of the future UV background, resulting in a self-consistent calculation of the coupled properties of the galaxy population and the IGM.

We use the formalism of Okamoto et al. (2008) to calculate the suppression of gas accretion due to photoheating, and the CLOUDY software to calculate the net cooling rate of the gas (i.e., cooling plus heating rates) inside halos. We allow for an additional *local* UV flux (i.e., over and above that of the metagalactic UV background) generated by the progenitors of the Milky Way. This results in an earlier effective redshift of reionization for the Milky Way and leads to further suppression of star formation in satellites, particularly in very low mass systems. However, in order to reionize the Universe sufficiently early, our model requires an escape fraction of UV photons of nearly 100%. This is higher than current observational estimates. Although these are uncertain, it seems likely that the high efficiency of photoionization required by our models may reflect either the limitations of the inevitable approximations we have made to calculate the reionization process or the neglect of other processes such as supernova-driven cosmic ray pressure which Wadepuhl & Springel (2011) argue could also play a role in suppressing galaxy formation in small halos.

We find that a model with supernova feedback as parameterized by Bower et al. (2006) predicts dwarf metallicities that are too low compared to observations. This can be rectified by assuming a lower efficiency of supernova feedback in small systems. We have found that a model with a saturation in the supernova feedback efficiency ($\beta =$ const) in dwarf satellite systems and with both local and global reionization provides the best match to the local luminosity function, the metallicity − luminosity relation, and the radial distribution and central densities of present day dwarf satellites. As it retains the default feedback efficiency for more massive systems, this model also matches the large-scale luminosity function.

In the fiducial model the suppression of faint satellites ($M_{\rm V} > -10$) is achieved by a combination of supernova feedback and (global+local) photoheating. However, the relative contribution of these processes varies across the range of dwarf galaxy sizes: supernova feedback is the dominant process for suppressing the more massive systems, photoheating plays the main role for the ultra-faint dwarfs.

While the role of reionization in suppressing galaxy formation in small halos has long been recognized, the importance of inhomogeneous reionization has only recently been highlighted (Busha et al. 2010; Muñoz et al. 2009). The local photoheating from Milky Way progenitors is a crucial ingredient in our model – unlike in most previous studies of the formation of satellites in the CDM cosmology, we find that global reionization by itself does not provide an acceptable solution to the 'missing satellite problem'. While the Bower et al. (2006) model gives a good match to the local luminosity function with global reionization only (see Fig. 4), it does not match the $Z - M_{\rm V}$ relation and produces too few dwarf satellites when local sources of reionization are taken into account. In contrast, the saturated feedback model matches all of these datasets well. Global reionization occurs at $z \approx 7.8$ and locally at $z \approx 10$.

In Appendix A, we show that reionization – with and without local photoheating – can be approximated using the standard $v_{\rm cut} - z_{\rm cut}$ rule (Benson et al. 2002b), but with parameters that differ from those typically adopted in other semi-analytical codes. For example, in the fbk:sat/rei:G model, the best fit is given by the set ($v_{\rm cut} = 34$ km s^{-1}, $z_{\rm cut} = 7.8$), and in the fbk:sat/rei:G+L model by the set ($v_{\rm cut} = 34$ km s^{-1}, $z_{\rm cut} = 10$). The $z_{\rm cut}$ values inferred this way are in very good agreement with the values derived from the full reionization treatment (see Fig. 3) and much less computationally intensive.

A more detailed comparison between our semi-analytical model and other models can be found in Section 4.5 and Appendix B. The model of Li et al. (2010) is the closest in methodology to the GALFORM model presented here and produces similar results.

The recent renewal of interest in the formation of satellite galaxies seems to be leading to a consensus that it is possible to reproduce basic properties of the galaxy population given *plausible* prescriptions for modelling reionization and its effects on galaxy formation (Busha et al. 2010; Koposov et al. 2009; Macciò et al. 2010; Busha et al. 2010; Li et al. 2010). Boylan-Kolchin et al. (2011), however, have recently presented dynamical evidence that the largest subhalos in ΛCDM N-body simulations are much too concentrated to be able to host the brightest satellites of the Milky Way. It is unclear at present whether this discrepancy could be due to statistics (Parry et al. 2011; dynamical data exist only for a handful of satellites in just one galaxy, the Milky Way) or whether it points to a more fundamental problem such as the existence of feedback processes not included in current models or even to a different nature for the dark matter (Lovell et al. 2011).

In this work, we have asked the general question of whether, in the context of the ΛCDM cosmology, it is possible to account for the observed properties of satellites not just *plausibly* but specifically within a broad model that has been developed to understand the galaxy population as a whole, not just the satellites. This is a more challenging question than merely constructing a model restricted to satellites, but one that provides a stronger test of our understanding of galaxy formation. We find, in agreement with earlier works, that a sufficiently high redshift of reionization, in combination with feedback from supernovae, can indeed reduce the number of satellites to a level which agrees with the data. The specificity of our model allows us to explore additional properties of satellites, such as their metallicity. We find that the metallicity-luminosity relation of satellites can only be explained at the same time as their luminosity function if supernova feedback saturates at low halo masses. Interestingly, our result raises the possibility that both the supernova feedback and reionization (global/local) are scale-dependent processes, which may have important consequences for our understanding of galaxy formation.

Like other recent models (Okamoto & Frenk 2009; Li et al. 2010), ours also provides an explanation for the apparent common mass scale of dwarf galaxies. In agreement with the conclusions of Stringer et al. (2010), we find that the weak dependence of M_{300} on L is a result of a weak dependence of M_{300} on M_{vir}. Our model predicts that there should, in fact, be a weak trend of increasing M_{300} with L and significant scatter in the relation at low luminosities. These predictions should be testable once improved measurements of M_{300} are available for larger samples of galaxies.

There have been significant and rapid advances over the past five years in both observations of dwarf satellites and our theoretical understanding of how they form. Despite this rapid progress, the conclusions of the previous generation of models remain essentially correct. The overall results seem independent of the details of any specific implementation of galaxy formation physics and lead to the conclusion that the broad visible properties of the satellite population are reproducible within the current cold dark matter paradigm. This represents an important success. Furthermore, the cold dark matter cosmogony makes clear predictions for the dark matter content of dwarf satellites that are mostly independent of the baryonic physics and are eminently testable by observations (Strigari et al. 2010; Boylan-Kolchin et al. 2011). An important challenge that remains for galaxy formation theory is to verify if the good agreement with dwarf satellite properties can be retained while simultaneously matching the broader properties of much more massive galaxies and galaxies at higher redshifts (see, for example, Guo et al. (2011a)). Given the complexity of galaxy formation it is only by confronting models with such a broad range of data that a convincing theory of galaxy formation will emerge.

ACKNOWLEDGEMENTS

We thank Gerry Gilmore for providing us the dwarf satellites metallicity data in Norris et al. (2010). ASF was supported by an STFC Fellowship at the Institute for Computational Cosmology in Durham and by a Royal Society Dorothy Hodgkin fellowship at the University of Cambridge. AJB acknowledges the support of the Gordon and Betty Moore Foundation. CSF acknowledges a Royal Society Wolfson Research Merit Award and ERC Advanced Investigator grant COSMIWAY. APC acknowledges an STFC studentship. GDL acknowledges financial support from the European Research Council under the European Community's Seventh Framework Programme (FP7/2007-2013)/ERC grant agreement n. 202781. AH acknowledges funding support from the European Research Council under ERC-StG grant GALACTICA-240271. Y-SL was supported by the Netherlands Organization for Scientific Research (NWO) STARE program 643.200.501. This work was supported in part by an STFC rolling grant to the Institute for Computational Cosmology of Durham University.

REFERENCES

Atek, H., Kunth, D., Schaerer, D., Hayes, M., Deharveng, J. M., Östlin, G., Mas-Hesse, J. M., 2009, A&A, 506, 1
Balogh, M. L., Navarro, J. F., Morris, S. 2000, ApJ, 540, 113
Battaglia, G., Helmi, A., Morrison, H., Harding, P., Olszewski, E. W., Mateo, M., Freeman, K. C., Norris, J., Shectman, S. A. 2006, MNRAS, 370, 1055
Battaglia, G. et al. 2006, A&A, 459, 423
Belokurov, V. et al. 2007, ApJ, 654, 897
Belokurov, V., Walker, M. G., Evans, N. W., Gilmore, G., Irwin, M. J., Mateo, M., Mayer, L., Olszewski, E., Bechtold, J., Pickering, T. 2009, 397, 1748
Benson, A. J., Lacey, C. G., Baugh, C. M., Cole, S., Frenk, C. S. 2002a, MNRAS, 333, 156

Benson, A. J., Frenk, C. S., Lacey, C. G., Baugh, C. M., Cole, S. 2002b, MNRAS, 333, 177

Benson, A. J., Sugiyama, N., Nusser, A., Lacey, C. G., 2006, MNRAS, 369, 1055

Benson, A. J., Bower, R. G. B. 2010, MNRAS, 405, 1573

Bolton, J. S., Haehnelt, M. G. 2007, MNRAS, 382, 325

Bower, R. G., Benson, A. J., Malbon, R., Helly, J. C., Frenk, C. S., Baugh, C. M., Cole, S., Lacey, C. G. 2006, MNRAS, 370, 645

Bower, R. G., McCarthy, I. G., Benson, A. J. 2008, MNRAS, 390, 1399

Boylan-Kolchin, M., Springel, V., White, S. D. M., Jenkins, A., Lemson, G. 2009, MNRAS, 398, 1150

Boylan-Kolchin, M., Springel, V., White, S. D. M., Jenkins, A. 2010, MNRAS, 406, 896

Boylan-Kolchin, M., Bullock, J. S., & Kaplinghat, M. 2011, arXiv:1103.0007

Bullock, J. S., Kravtsov, A. V. & Weinberg, D. H.2000, ApJ, 539, 517

Busha, M. T., Alvarez, M. A., Wechsler, R. H., Abel, T., Strigari, L. E. 2010, ApJ, 710, 408

Cole, S., Lacey, C. G., Baugh, C. M., Frenk C. S., 2000, MNRAS, 319, 168

Cole S. et al., 2001, MNRAS, 326, 255

Cooper, A. P. et al. 2010 MNRAS, 406, 744

Couchman, H. M. P., Rees, M. J. 1986, MNRAS, 221, 53

Croton, D. J., Springel, V., White, S. D. M., De Lucia, G., Frenk, C. S., Gao, L., Jenkins, A., Kauffmann, G., Navarro, J. F., Yoshida, N. 2006, MNRAS, 365, 11

Da Costa, G. S., Freeman, K. C., Kalnajs, A. J., Rodgers, A. W., & Stapinski, T. E. 1977, AJ, 82, 810

Dekel, A. & Silk, J. 1986, ApJ, 303, 39

De Lucia, G., Kauffmann, G., White, S. D. M. 2004, MNRAS, 349, 1101

De Lucia, G. & Blaizot, J. 2007, MNRAS, 375, 2

De Lucia, G. & Helmi, A. 2008, MNRAS, 391, 14

De Lucia, G., Boylan-Kolchin, M., Benson, A. J., Fontanot, F., Monaco, P. 2010, MNRAS, 406, 1533

Diemand, J., Kuhlen, M., Madau, P. 2007, ApJ, 657, 262

Efstathiou, G. 1992, MNRAS, 256, 43

Ferland, G. J., Korista, K. T., Verner, D. A., Ferguson, J. W., Kingdon, J. B., Verner, E. M. 1998, PASP, 110, 761

Fernandez, E. R., Shull, J. M. 2011, ApJ, 731, 20

Flynn, C., Holmberg, J., Portinari, L., Fuchs, B., Jahreiß, H., 2006, MNRAS, 372, 1149

Font, A. S., Bower, R. G., McCarthy, I. G., Benson, A. J., Frenk, C. S., Helly, J. C., Lacey, C. G., Baugh, C. M., Cole, S. 2008, MNRAS, 389, 1619

Gilmore, G. et al. 2007, ApJ, 663, 948

Gnedin, N. Y. 2000, ApJ, 542, 535

Guo, Q. et al., 2011, MNRAS, 413, 101

Guo Q., Cole S., Eke V., Frenk C., 2011, arXiv, arXiv:1101.2674

Haardt, F. & Madau, P. 1996, ApJ, 461, 20

Haardt, F. & Madau, P. 2001, in Proceedings of "Clusters of Galaxies and the High Redshift Universe Observed in X-rays", eds. Neumann, D. M. and Tran, J. T. V., 2001cghr.confE..64H

Harker, G., Cole, S., Helly, J. C., Frenk, C. S., Jenkins, A. 2006, MNRAS, 367, 1039

Helly, J. C., Cole, S., Frenk, C. S., Baugh, C. M., Benson, A. J., Lacey, C. 2003, MNRAS, 338, 903

Helmi, A. et al. 2006, 651, L121

Hoeft, M., Yepes, G., Gottlöber, S., Springel, V. 2006, MNRAS, 371, 401

Iliev, I. T., Moore, B., Gottlöber, S., Yepes, G., Hoffman, Y. 2011, Mellema, G. MNRAS, 413, 2093

Irwin, M. J. et al. 2007, ApJL, 656, L13

Kauffmann, G., White, S. D. M., & Guiderdoni, B. 1993, MNRAS, 264, 201

Kirby, E. N., Simon, J. D., Geha, M., Guhathakurta, P., Frebel, A. 2008, ApJL, 685, L43

Kirby, E. N., Lanfranchi, G. A., Simon, J. D., Cohen, J. G., Guhathakurta, P. 2011, ApJ, 727, 78

Klypin, A., Kravtsov, A. V., Valenzuela, O., Prada, F. 1999, ApJ, 522, 82

Komatsu E., et al., 2011, ApJS, 192, 18

Koposov, S. E., Belokurov, V., Evans, N. W., Hewett, P. C., Irwin, M. J., Gilmore, G., Zucker, D. B., Rix, H.-W., Fellhauer, M., Bell, E. F., Glushkova, E. V. 2008, ApJ, 686, 279

Koposov, S. E., Yoo, J., Rix, H.-W., Weinberg, D. H., Macciò, A. V.; Escudé, J. M. 2009, ApJ, 696, 2179

Kravtsov, A. V., Gnedin, O. Y., Klypin, A. A. 2004, ApJ, 609, 482

Larson, R. B., Tinsley, B. M., Caldwell, C. N. 1980, ApJ, 237, 692

Laursen, P., Sommer-Larsen, J., Andersen, A. C., 2009, ApJ, 704, 1640

Letarte, B. et al. 2010, A&A, 523, L17

Li, Y.-S. Helmi, A., De Lucia, G., Stoehr, F. 2009, MNRAS, 397, 87L

Li, Y.-S., De Lucia, G., Helmi, A. 2010, MNRAS, 401, 2036

Liu L., Gerke B. F., Wechsler R. H., Behroozi P. S., Busha M. T. 2011, ApJ, 733, 62

Libeskind, N. I., Cole, S., Frenk, C. S., Okamoto, T., Jenkins, A. 2007, MNRAS, 374, 16L

Lovell, M., et al. 2011, arXiv:1104.2929

Macciò, A. V., Kang, X., Moore, B. 2009, ApJL, 692, 109

Macciò, A. V., Kang, X., Fontanot, F., Somerville, R. S., Koposov, S. E., Monaco, P. 2010, MNRAS, 402, 1995

Martin, N. F., Ibata, R. A., Bellazzini, M., Irwin, M. J., Lewis, G. F., & Dehnen, W. 2004, MNRAS, 348, 12

Martin, N. F., de Jong, J. T. T., & Rix, H. -W. 2008, MNRAS, ApJ, 684, 1075

Mateo, M. 1998, ARA&A, 36, 435

Mesinger, A., Furlanetto, S., Cen, R., 2011, MNRAS, 411, 955

McCarthy, I. G., Frenk, C. S., Font, A. S., Lacey, C. G., Bower, R. G., Mitchell, N. L., Balogh, M. L., Theuns, T. 2008, MNRAS, 383, 593

Mo, H., White, S. D. M., 1996, MNRAS, 282, 347

Moore, B., Ghigna, S., Governato, F., Lake, G., Quinn, T., Stadel, J., Tozzi, P. 1999, ApJ, 524, 19

Moore, B., Diemand, J., Madau, P., Zemp, M., Stadel, J. 2006, MNRAS, 368, 563

Muñoz, J. A., Madau, P. Loeb, A., Diemand, J. 2009, MNRAS, 400, 1593

Navarro, J. F., Frenk, C. S., & White, S. D. M. 1996, ApJ, 462, 563

Navarro, J. F., Frenk, C. S., & White, S. D. M. 1997, ApJ, 490, 493

Neto, A. F., Gao, L., Bett, P., Cole, S., Navarro, J. F., Frenk, C. S., White, S. D. M., Springel, V., Jenkins, A.

2007, MNRAS, 381, 1450
Norris, J. E., Wyse, R. F. G., Gilmore, G., Yong, D. Frebel, A., Wilkinson, M. I., Belokurov, V., Zucker, D. B. 2010, ApJ, 723, 1632
Okamoto, T., Gao, L., Theuns, T. 2008, MNRAS, 390, 920
Okamoto T., Frenk C. S., 2009, MNRAS, 399, L174
Okamoto T., Frenk C. S., Jenkins A., Theuns T., 2010, MNRAS, 406, 208
Parkinson, H., Cole, S., Helly, J., 2008, MNRAS, 383, 557
Parry, O. H., Eke, V. R., Frenk, C. S., & Okamoto, T. 2011, arXiv:1105.3474
Press, W. H., Schechter, P. 1974, ApJ, 187, 425
Raicevic, M., Theuns, T., Lacey, C. 2011, MNRAS, 410, 775
Salvadori, S., Ferrara, A. 2009, MNRAS, 395, L6
Siana, B., Teplitz, H. I., Colbert, J., Ferguson, H. C., Dickinson, M., Brown, T. M., Conselice, C. J., de Mello, D. F., Gardner, J. P., Giavalisco, M., Menanteau, F., 2007, ApJ, 668, 62
Smith, M. C. et al. 2007, MNRAS, 379, 755
Somerville, R. S. 2002, ApJ, 572, 23
Springel, V., White, Simon D. M., Tormen, G., Kauffmann, G. 2001, MNRAS, 328, 726
Springel, V. 2005a, MNRAS, 364, 1105
Springel, V. et al. 2005b, Nature, 435, 629
Springel, V., et al. 2008, Nature, 456, 73
Springel, V., et al. 2008, MNRAS, 391, 1685
Stark D. P., Ellis R. S., Chiu K., Ouchi M., Bunker A., 2010, MNRAS, 408, 1628
Strigari, L. E., Frenk, C. S., & White, S. D. M. 2010, MNRAS, 408, 2364
Strigari, L. E., Koushiappas, S. M., Bullock, J. S., Kaplinghat, M., Simon, J. D., Geha, M., Willman, B. 2008, ApJ, 678, 614
Stringer, M., Cole, S., & Frenk, C. 2010, MNRAS, 404, 1129
Thoul A. A., Weinberg D. H., 1996, ApJ, 465, 608
Tollerud, E. J., Bullock, J. S., Strigari, L. E., & Willman, B. 2008, ApJ, 688, 277
Vanzella, E. et al. 2010, ApJ, 725, 1011
Wadepuhl M., Springel V., 2011, MNRAS, 410, 1975
Walsh, S. M., Jerjen, H., & Willman, B. 2007, ApJ, 662, L83
Walker, M. G., Mateo, M., Olszewski, E. W., Peñarrubia, J., Wyn, E. N., Gilmore, G. 2010, ApJ, 710, 886
Wang, J., De Lucia, G., Kitzbichler, M. G., & White, S. D. M. 2008, MNRAS, 384, 1301
Weinmann, S. M., Macciò, A. V., Iliev, I. T., Mellema, G., Moore, B. 2007, MNRAS, 381, 367
White, S. D. M. & Frenk, C. S. 1991, ApJ, 379, 52
White S. D. M., Rees M. J., 1978, MNRAS, 183, 341
Willman, B. et al. 2005, ApJL, 626, L85
Wise, J. H., Cen, R., 2009, ApJ, 693, 984
Wise, J. H., Turk, M. J., Norman, M. L., Abel, T., 2010, arXiv1011.2632
Wolf, J., Martinez, G. D., Bullock, J. S., Kaplinghat, M., Geha, M., Munoz, R. R., Simon, J. D., & Avedo, F. F. 2010, MNRAS, 406, 1220
Xue, X. X. et al. 2008, ApJ, 684, 1143
Zucker, D. B. et al. 2006, ApJL, 643, L103

APPENDIX A: THE $(V_{\rm CUT}, Z_{\rm CUT})$ APPROXIMATION

A self-consistent calculation of reionization in GALFORM was described by Benson et al. (2002a), who showed that this calculation is well approximated by the $(v_{\rm cut},\ z_{\rm cut})$ model used subsequently in the GALFORM code. In this approximation, the baryon fraction accreted by halos is given by:

$$f_{\rm b} = \begin{cases} 0 & \text{if } z < z_{\rm cut} \text{ and } v_{\rm vir} < v_{\rm cut}, \\ \langle f_{\rm b} \rangle & \text{otherwise}, \end{cases} \qquad (5)$$

where $\langle f_{\rm b} \rangle$ is the mean cosmic baryon fraction. This 'shortcut' greatly speeds up the semi-analytic code. It has been adopted in several other semi-analytic models such as those by Bullock, Kravtsov & Weinberg (2000) and Somerville (2002). It is therefore interesting to check whether the new treatment of reionization implemented in this paper is still well approximated by a step function of the form above, and if so, to determine the best fit values of the $(v_{\rm cut}, z_{\rm cut})$ parameters.

We find that the simple $(v_{\rm cut}, z_{\rm cut})$ model still provides a good approximation to the full calculation of reionization even when local sources as included. We illustrate this with the fbk:sat model, although this conclusion is equally valid for other feedback schemes, including the default power-law feedback scheme, fbk:B06.

Fig. 13 shows the $(v_{\rm cut}, z_{\rm cut})$ approximation for the models with saturated feedback and self-consistent global reionization, with or without local reionization, fbk:sat/rei:G and fbk:sat/rei:G+L, assuming an escape fraction of ionizing photons of 100%. The luminosity functions are shown with different colours, each one corresponding to one of the six Aquarius halos.

We find that the parameter values $(v_{\rm cut}, z_{\rm cut}) =$ (34 km s^{-1}, 7.8) provide a good match to the model with global emission only, fbk:sat/rei:G. The best fit $v_{\rm cut}$ is slightly higher than the critical circular velocity of 25 km s^{-1} obtained for the Okamoto, Gao, & Theuns (2008) accretion model. This is because in GALFORM photoheating not only prevents accretion onto halos below some mass but it also offsets radiative cooling losses (and therefore star formation rates) for systems that are massive enough to accrete baryons). Note that z_{cut} gives a very good approximation to the redshift of reionization calculated self-consistently (see Fig. 3).

Adding the ionizing flux from the local sources turns out to be equivalent to shifting the redshift of reionization to earlier values, while keeping $v_{\rm cut}$ roughly constant. The best $(v_{\rm cut}, z_{\rm cut})$ approximation for the fbk:sat/rei:G+L case is $(v_{\rm cut}, z_{\rm cut}) =$ (34 km s^{-1}, 10).

We find that similar good $(v_{\rm cut}, z_{\rm cut})$ approximations exist for the other cases when $f_{\rm esc}$ is varied. Perhaps more surprisingly, we find that the $(v_{\rm cut}, z_{\rm cut})$ approximation works well for a variety of other feedback schemes (including the default fbk:B06 and power-laws with varying slopes), regardless or whether or not a local photoionizing flux is included, and irrespective of the variety of merger histories represented in the Aquarius halos. It is also surprising that the approximation works quite well down to the regime of the ultra-faint dwarfs, even though it was first derived in the regime of classical dwarfs. The success of this approx-

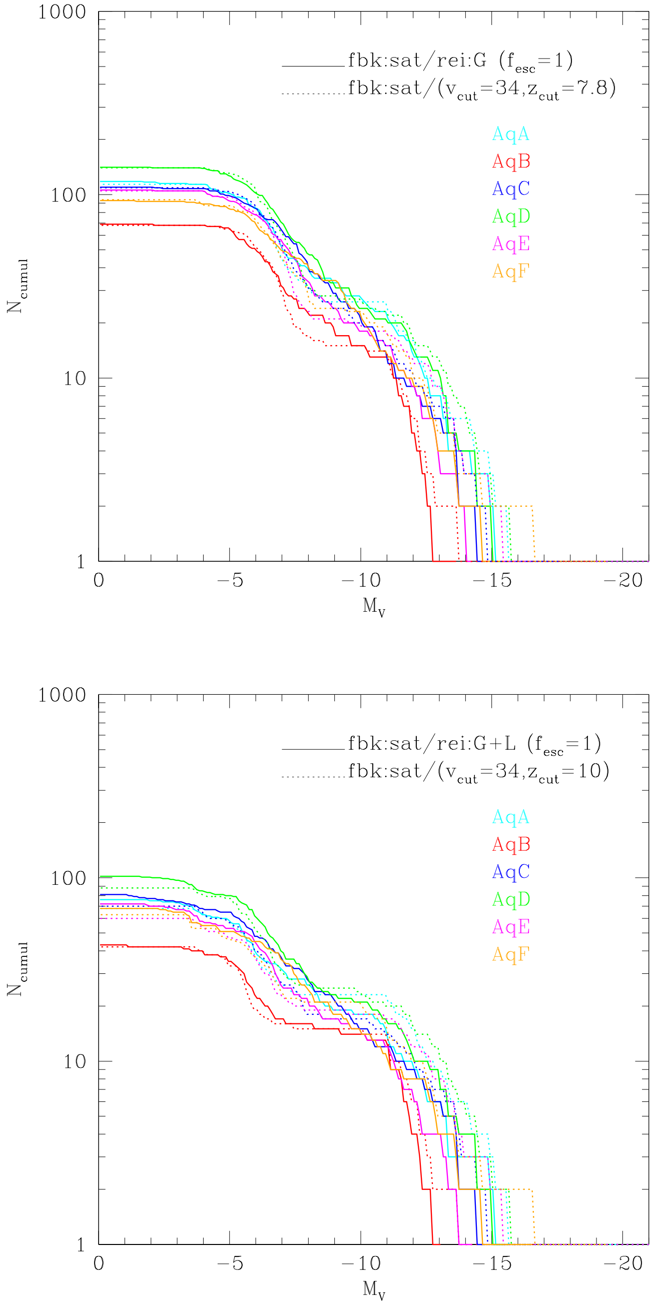

Figure 13. Comparison between the models with a detailed calculation of reionization and the $(v_{\rm cut}, z_{\rm cut})$ approximation. Full lines represent fbk:sat/rei:G models in the top panel and fbk:sat/rei:G+L models in the bottom panel, respectively. The various colours correspond to the six Aquarius halos. Dotted lines in both top and bottom panels represent the models with the $(v_{\rm cut}, z_{\rm cut})$ approximation. The values for this pair of parameters are: $(v_{\rm cut}, z_{\rm cut})$=(34 km s^{-1}, 7.8) in the top panel and $(v_{\rm cut}, z_{\rm cut})$=(34 km s^{-1}, 10) in the bottom panel.

imation could not have been predicted *a priori*, given the differences between our current models and those of the original Benson et al. (2002a) model where the approximation was introduced.

APPENDIX B: COMPARISON WITH OTHER MODELS

Several other studies of Milky Way satellite galaxies in the context of the cold dark matter cosmogony have recently been carried out. The broad consensus from these investigations is that theoretical models can achieve agreement with the observed distribution of satellite galaxy luminosities given reasonable assumptions about the process of star formation and the ability of the reionization of the Universe to suppress galaxy formation in low mass halos. These studies have included various pieces of physics thought to be relevant to the formation of low mass galaxies, but none have performed as detailed and physically complete calculations as described in this work. Below we briefly outline the methods and results of these recent works and contrast them with our own.

5.1 Busha et al. (2010)

Busha et al. (2010) explored the effects of inhomogeneous reionization on the population of Milky Way satellites using a combination of a high-resolution N-body simulation of the Milky Way halo and a lower resolution, larger volume simulation of the universe to assess spatial variations in the epoch of reionization. They find that reionization typically occurs between $z = 6$ and $z = 12$ for Milky Way-sized halos. To model the formation of galaxies within their dark matter only simulation, Busha et al. (2010) assume that halos must have reached a critical mass (corresponding to the atomic cooling limit of approximately 10^4K) prior to reionization. They then assign luminosities to galaxies using one of two methods. In the first, the assume a one-to-one mapping between luminosity and peak halo velocity, $v_{\rm max}$. In the second, more physically motivated approach, a star formation rate proportional to a power of the halo mass is assigned to each halo between the time it reaches the critical mass and the epoch of reionization. The luminosity is found by applying a stellar population synthesis model and integrating over this star formation rate.

Busha et al. (2010) find that, with a suitable choice of star formation rate normalization, the second model produces a good match to the faint end of the observed satellite luminosity function. (The bright end is underpredicted, but this is understandable as they do not allow for star formation in massive halos after reionization.) Additionally, they find that their model produces a good match to the radial distribution of satellites while simultaneously producing values of M_{300} in reasonable agreement with the data (although somewhat too high for the more luminous halos).

In comparison to our treatment, the model of Busha et al. (2010) is much more simplistic. However, their results agree with ours at a qualitative level – sufficiently early reionization can reduce the number of satellites to a level compatible with observations. Additionally, their conclusion that the abundance of satellites is very sensitive to the epoch of reionization is consistent with our findings. For this reason, Busha et al. (2010) emphasize the importance of considering inhomogeneous reionization, consistent with our finding that localized ionization from progenitors of the Milky Way plays a key role in setting the local reionization epoch. Busha et al. (2010) use the Via Lactea II simulation which has a halo mass of $2.6\times10^{12}M_{\odot}$, somewhat more massive than the halos considered here, but do not address the issue of whether their model produces a Milky Way galaxy with the correct properties (such as stellar mass).

5.2 Muñoz et al. (2009)

Muñoz et al. (2009) adopt a slightly more involved approach, also utilizing the Via Lactea II N-body simulation. They consider four channels of star formation. In low mass halos at early times they allow stars to form via molecular hydrogen cooling. This process is stopped at $z = 20$ when molecular hydrogen is assumed to be dissociated. Prior to reionization at $z \sim 11$, stars are allowed to form in halos above the atomic cooling limit, while after reionization, star formation is restricted to higher mass halos. At late times, some further star formation resulting from metal line cooling is allowed. In each case, a simple parameterization is employed in which the mass of stars formed is proportional to the mass of the halo during the relevant epoch. Stellar population synthesis models are then used to infer galaxy luminosities.

With a suitable choice of parameters, Muñoz et al. (2009) find excellent agreement with the observed satellite luminosity function and show that molecular hydrogen cooling is important for producing the correct abundance of low luminosity satellites. They additionally explore the behaviour of M_{300} as a function of luminosity and find broadly good agreement with the data although with significantly more scatter than observed and a trend for M_{300} to be too high in bright galaxies and too low in faint galaxies.

The work of Muñoz et al. (2009) contains many of the features of our own work (e.g., H_2 cooling and the effect of photons generated locally). Our model, however, includes a rigorous treatment of the variety of physical process involved in galaxy formation such as gas cooling, star formation, feedback and global reionization which have been tested against observations of the galaxy population as a whole at different redshifts. It is unclear whether the *ad hoc* prescriptions of Muñoz et al. (2009) would lead to realistic galaxies beyond the satellites of the Milky Way.

5.3 Koposov et al. (2009)

The study by Koposov et al. (2009) differs from other studies in that it employs a semi-analytic method to follow the growth and evolution of the subhalo population inside a halo of final mass $10^{12}M_{\odot}$. As we discussed above, it is possible that this mass may be too small for the Milky Way halo. However, like most other studies, Koposov et al. (2009) do not explore whether their model produces a central galaxy with a stellar mass comparable to that of the Milky Way. They explore a variety of prescriptions for assigning stars to subhalos, including simple models in which a constant fraction of baryons turns into stars and models in which stars can only form in halos above some critical characteristic velocity after the epoch of reionization at $z = 11$ (either with a sharp transition from star forming to non-star forming at this critical velocity, or a smoother transition motivated by the work of Gnedin (2000)).

They find that the faint end of the luminosity function is made up of galaxies which formed their stars before the epoch of reionization, with brighter satellites forming in more massive halos after reionization. In fact, in their models with a sharp transition at the critical velocity they see a bimodal luminosity function made up of these two types of galaxy. In models with a smooth transition the bimodality is lost and good agreement with the observed luminosity function is obtained. Their results for M_{300} are consistent with those of other works (although with less scatter – a consequence of their neglect of scatter in the mass-concentration relation, as they note).

The approach of Koposov et al. (2009) is significantly more phenomenological than that described in this work, but it helps to confirm, as do other works, that an early epoch of reionization can plausibly suppress dwarf galaxy formation sufficiently to achieve agreement with the observations.

5.4 Macciò et al. (2010)

Macciò et al. (2010) compare results from three different semi-analytic models of galaxy formation applied to high-resolution N-body simulations. Their halos span masses from 1.2 to $3.6\times10^{12}M_{\odot}$ with a median of $1.7\times10^{12}M_{\odot}$, and so they could potentially suffer from the same shortcoming as the Aquarius halos of being of somewhat too low mass. Their semi-analytic models have been previously matched to the properties of the broader population of galaxies, but unfortunately, they do not specify whether or not they produce the correct mass of the central galaxy in these halos.

In contrast to our approach, the subhalo information is not used to determine the evolution of satellite galaxies (e.g. to determine merging timescales). To add a suitable reionization-induced suppression of galaxy formation, the Gnedin (2000) filtering mass prescription is added to each model, with a reionization history taken from Kravtsov et al. (2004). They find that all three models can achieve a reasonable match to the observed satellite luminosity function with a reionization epoch of $z = 7.5$. However, they note that the original filtering mass prescription overestimates the suppressing effects of reionization. Adopting the currently favoured suppression (which becomes effective in halos with characteristic velocities below ~ 30 km s^{-1}), they find that a higher redshift, $z = 11$, of reionization is required to restore a good match to the data. Macciò et al. (2010) explore the roles of various physical ingredients in their models in achieving this match. In particular, and in agreement with this work, they find that the inclusion of supernova feedback is crucially important – without it far too many luminous galaxies are formed.

The work of Macciò et al. (2010) is closest to our own in terms of the range of physics modelled and the detail of the treatment. However, these models lack the potentially important effects of molecular hydrogen cooling and do not include of a self-consistently computed reionization history.

5.5 Guo et al. (2010)

Guo et al. (2011a) use a semi-analytic model of galaxy formation to study the properties of galaxies in dark matter halos spanning a wide range of scales by utilizing dark matter halo merger trees from the Millennium and Millennium-II N-body simulations. Subhalo information is taken from the simulations and used to track the merging of satellite galaxies. Of relevance to this work, their Millennium-II merger trees resolve halos down to a mass of approximately $2 \times 10^8 M_\odot$, which is sufficient to just resolve Milky Way dwarf satellites. To study Milky Way analogues, Guo et al. (2011a) select halos from the Millennium-II simulation which contain a disk-dominated (judged in terms of stellar mass) central galaxy with a total stellar mass in the range $4 \times 10^{10} M_\odot < M_\star < 6 \times 10^{10} M_\odot$ which results in a median halo mass of $1.44 \times 10^{12} M_\odot$. This once again raises the potential issue of the halo masses being too small, although in this case if further observational evidence suggests a higher mass for the Milky Way halo it would necessitate a recalibration of the Guo et al. (2011a) galaxy formation model to reduce the stellar mass of galaxies in dark matter halos of given mass. The galaxy formation models used are based on models previously used to successfully model various aspects of the galaxy population. Importantly, Guo et al. (2011a) explore how their model performs not only for the Milky Way satellite population, but also for the broader population of galaxies. They demonstrate that their model provides a good match to field and cluster galaxy luminosity functions while simultaneously matching that of Milky Way satellites.

The key physics of reionization is incorporated into the model of Guo et al. (2011a) in by use of the Gnedin (2000) filtering mass prescription, with a filtering mass as a function of redshift extracted from the simulations of Okamoto et al. (2008). Guo et al. (2011a) find that they obtain good agreement with the luminosity function of Milky Way satellites using their standard reionization prescription correctly predicts the number of bright satellites, but is marginally inconsistent with the number of faint satellites (producing somewhat too many, although the model remains plausible given current uncertainties in the observational sample). They find that removing the effects of reionization only affects the abundance of fainter galaxies. Although Guo et al. (2011a) do not discuss this point, this implies that supernovae feedback plays a major role in inhibiting the formation of satellite galaxies, in agreement with our own findings.